Microporous and Mesoporous Materials 236 (2016) 141–157

Contents lists available at ScienceDirect

Microporous and Mesoporous Materials

journal homepage: www.elsevier.com/locate/micromeso

Review

Stimuli-responsive mesoporous silica nanoparticles for cancer therapy: A review

André F. Moreira, Diana R. Dias, Ilídio J. Correia*

CICS-UBI – Health Sciences Research Centre, Universidade da Beira Interior, Av. Infante D. Henrique, 6200-506 Covilhã, Portugal

ARTICLE INFO

Article history:
Received 19 July 2016
Received in revised form
29 August 2016
Accepted 30 August 2016
Available online 31 August 2016

Keywords:
Cancer therapy
Drug delivery
Mesoporous silica nanoparticles
Stimuli-responsive behavior

ABSTRACT

The application of nanocarriers as selective drug delivery platforms, as imaging or as diagnostic agents has been evaluated in several studies in the area of biomedicine, namely for cancer therapy. Such systems have the potential to perform a controlled and site-specific delivery of therapeutic agents leading to a reduction of side effects and, ultimately, to an improved therapeutic outcome. Among the different nanocarriers developed so far, mesoporous silica nanoparticles have attracted the attention of the scientific community for being applied as drug delivery systems that are capable of controlling, both in space and time, the drug release. In this review, the modifications performed, so far, on mesoporous silica nanoparticles to imprint them a stimulus responsive behavior (namely, pH, redox potential, adenosine triphosphate, enzyme or temperature) in order to allow their application in cancer therapy are highlighted.

1. Introduction

The developments achieved in the area of nanotechnology in the past decades allowed the production of various nano-sized platforms, such as drug/gene delivery systems (DDSs) [1], biosensors [2], biomarkers [3] and imaging [4] that are currently being applied in different areas like electronics and medicine. Particularly, the enhanced properties displayed by the nano-sized platforms prompted their application in the transport and delivery of specific drugs to treat diseases such as cancer [5], Alzheimer [6] and Parkinson [7]. Particularly, in cancer therapy, the DDSs can have a huge impact on the therapeutic outcome attained with conventional chemotherapies [8]. Nano-sized carriers such as liposomes, dendrimers, polymeric and inorganic carriers can be used to encapsulate poorly soluble anti-cancer drugs, protect them from premature degradation in the body, and also decrease their interaction with healthy tissues, thus reducing side effects. Furthermore, the DDSs take advantage of their reduced size and specific surface properties to effectively accumulate in tumor tissue, through a process that exploits the abnormal vasculature of the tumor, i.e., the enhanced permeability and retention effect (EPR) (passive targeting) [9]. Moreover, the functionalization of DDSs with targeting ligands (active targeting) allow them to interact with specific cells thus reducing the nonspecific tissue biodistribution [10–12]. Another important aspect that has to be taken into account in the design and production of nano-sized DDSs is their capacity to perform a controlled release at the tumor site in response to a specific stimulus [13].

The DDSs can be produced with a wide number of different organic and inorganic materials including natural and synthetic polymers, lipids, self-assembling amphiphilic molecules, metals and other inorganic materials [14]. The raw material selection is highly influenced by the pretended application in which the nanoparticles will be enrolled in (imaging, therapy, diagnostic or theranostics), the cargo characteristics, the material biocompatibility and the desired route of administration. Several different DDSs based on organic materials have already been assayed in clinical trials, although only a few were approved by the Food and Drug Administration (FDA) for cancer therapy (e.g. Abraxane®, DaunoXome® and Doxil®). On the other side, most of the nanocarriers based on inorganic materials are still in preclinical or basic research development phase. Among them, gold and silica nanoparticles are an exception, since they received the FDA approval to be assayed in clinical trials for cancer therapy or imaging applications [15].

The silica nanoparticles, especially those with mesopores, have attracted the interest of the scientific community due to their potential to be applied in the nanomedicine field. The main

* Corresponding author.
E-mail address: icorreia@ubi.pt (I.J. Correia).

http://dx.doi.org/10.1016/j.micromeso.2016.08.038
1387-1811/

Abbreviation list

AP	3-aminopropyl
ATP	Adenosine triphosphate
BA	Bafilomycin A1
CTAB	Hexadecyltrimethylammonium bromide
DDSs	Drug delivery systems
Dox	Doxorubicin
DTT	Dithiothreitol
EPR	Enhanced permeation and retention effect
FAP	N-folate-3-aminopropyl
FDA	Food and Drug Administration
FITC	Fluorescein isothiocyanate
GEGP	3-[N-(2-guanidinoethyl) guanidino]propyl
GP	Guanidinopropyl
GSH	Glutathione
MMP	Matrix metalloproteinase
MSNs	Mesoporous silica nanoparticles
NIR	Near infrared
PEG	Poly (ethylene glycol)
PHEMA	Poly (2-hydroxyethyl methacrylate)
PVP	Poly (2-vinylpyridine)
RBCs	Red blood cells
RES	Reticuloendothelial system
RGD	Arg-Gly-Asp
ROS	Reactive oxygen species
SMCC	Succinimidyl 4-N-maleimidomethyl cyclohexane-1-carboxylate
S-NPs	Ultra-small lanthanide doped nanoparticles with ultra-thin TaOx layer
TEOS	Tetraethyl orthosilicate
TMOS	Tetramethyl orthosilicate
Zn-Por-CA-PEG	PEGylated tetraphenylporphyrin zinc

advantages of mesoporous silica nanoparticles (MSNs) arise from its simple, scalable, and cost-effective fabrication as well as its non-toxic matrix structure, large pore volume and surface area that is prone to be functionalized [16,17]. Furthermore, the tubular pores presented by MSNs increase their drug loading capacity, which is fundamental to avoid drug degradation during administration and blood circulation [18]. Moreover, the combination of the tubular pores and the high number of silanol groups present on particle's surface allow the use of various gatekeepers (e.g. polymers, nanoparticles or small molecules) to seal the cargo loaded on MSNs [19–21].

In recent years, MSNs development included structure design, biosafety profile characterization, biodistribution and mechanisms of excretion studies [22–25]. Herein, the recent progress on the development of stimuli-responsive MSNs for cancer treatment are summarized, focusing on the different modification performed on MSNs to imprint them a stimuli-responsive character (e.g. pH, redox, adenosine triphosphate (ATP), enzyme, and temperature).

2. Mesoporous silica nanoparticles

The synthesis of monodispersed silica particles involves a sol-gel method that was reported for the first time by Stöber et al. in 1968. Such method involves the hydrolysis of tetraalkyl silicates in an alcohol and water solution using ammonia as a catalyst, to originate non-porous silica particles that can be engineered to possess sizes in the range of a few nanometers to some microns [26]. MSNs were initially synthesized through a modification of the method described above, by using micelles formed by cationic surfactants, like hexadecyltrimethylammonium bromide (CTAB), that act as the templating agents for the formation of particle mesopores [27]. To accomplish that the silica precursor (tetramethyl orthosilicate (TMOS), tetraethyl orthosilicate (TEOS) or other) is added into a heated basic solution containing CTAB. Then, occurs the base-catalyzed hydrolysis of the silica precursor, since the OH^- groups present in solution attack this molecule (TMOS or TEOS) through a nucleophilic attack mechanism [28]. This reaction will promote the removal of the alkoxy group ($O-CH_2-CH_3$ in TEOS case) allowing the condensation of these molecules via siloxane bonds (Si–O–Si) at the surface of surfactant micelles [28]. Such process occurs through the electrostatic interactions between the cationic surfactant template and the negatively charged silica species, leading to the formation of a silica wall and by the combination of these structures the MSNs are formed [29]. For a detailed review of the MSNs synthesis procedures the readers are referred to [29].

The MSNs, particularly the MCM-41 type, are characterized by their honeycomb-like porous structure that has a large number of empty channels (mesopores) that run from one end of the structure to the other without showing interconnections. They also possess unique properties such as a tunable particle size, stable and rigid framework, a high surface area (>700 m^2/g), large pore volume (>0.6 cm^3/g), uniform and adjustable pore size (2–10 nm) and good chemical and thermal stability [30,31]. When compared to the organic nanocarriers, MSNs are more resistant to pH, temperature variations and also to mechanical stress, which renders them an improved capacity to protect the drug cargo when in contact with body fluids [32]. Moreover, the large pore volume and tunable pore sizes displayed by MSNs allow the incorporation of bioactive molecules with a higher efficiency [16]. Drugs, genes or proteins are usually loaded in MSNs by immersing them in solutions containing the therapeutic molecules [33]. In this process, the therapeutic molecules are encapsulated in the MSNs matrix by adsorption, a process that involves the formation of hydrogen bonds or electrostatic interactions between the cargo molecules and the MSNs [34]. The loading process can be further enhanced by using a solvent evaporation method, employing cycles of impregnation and evaporation that are fundamental to promote the drug diffusion into the pores by capillarity, and ultimately increase the loading efficiency [35]. Moreover, since MSNs can endure the exposition to organic solvents, the appropriate solvent can be chosen to attain a complete solubilization of the therapeutic molecule leading to an increased drug encapsulation efficiency. The MSNs pore size is another important parameter that greatly influence the particles capacity to adsorb specific therapeutic molecules. The MSNs pores usually have a diameter of 2–4 nm, which impairs the loading of larger molecules, although in literature different reports have been showing that it is possible to tune the pore sizes up to 30 nm by using quaternary ammonium surfactants with different lengths or even polymers (e.g. Pluronic F127) [36,37]. Such modifications allow the encapsulation of a wide number of molecules, spawning from small drugs to larger DNA molecules or proteins [38,39].

On the other side, due to the silanol groups present on MSNs surface, the functionalization of MSNs with different molecules can occur either by covalent bonding or through electrostatic interactions [40]. The covalent grafting of functional moieties usually

involves, in a first step, the introduction of silane modified materials using co-condensation or post-synthetic grafting methods [41]. The co-condensation method relies on the hydrolysis of the silane modified materials while the MSNs are forming, allowing the incorporation of the functional moieties in the resultant silica structure. On the other hand, post-synthetic grafting methods are performed after the MSNs synthesis (before or after the pore template removal) to add the functional groups mainly on MSNs surface. Alternatively, the functional moieties can also be introduced on the MSNs through electrostatic interactions. Such process takes advantage of the negatively charged silanol groups available on MSNs surface that can interact with the positively charged groups present in the functional moieties, resulting in the adsorption of these molecules on MSNs surface. MSNs functionalization can be used to improve particle biocompatibility, tumor accumulation or to restrain the uncontrolled pre-leakage of therapeutic agents before they arrive to tumor site [42–44].

3. MSNs application in cancer therapy

Surgery, radiotherapy, chemotherapy or their combination are still the most used therapeutic approaches used for cancer therapy. In chemotherapy, the administration of highly cytotoxic drugs is hindered by their low water solubility, rapid degradation, decreased bioavailability and lack of specificity, which is responsible for severe side effects [45–47]. Such features highlight the limitations of anti-cancer drugs used nowadays in the clinic, since there are constraints relatively to the maximum dose and number of treatments that can be administered to each patient [19]. In fact, such dose restriction in conjugation with a decreased bioavailability, usually, results in a lower therapeutic outcome and can trigger the development of resistance to these therapies by cancer cells [48]. Therefore, it is crucial to develop carriers that are capable of protecting the drugs and deliver them in a spatial and temporally controlled fashion that improve their therapeutic outcome. In the last decade, MSNs for anti-cancer purposes have been used in a huge number of studies (please see Fig. 1). These nanoparticles were tested as diagnostic systems (fluorescence imaging or magnetic resonance imaging), therapeutic devices (drug delivery or photothermal therapy), or even as theranostics agents (single nanocarriers that are capable of combining the diagnostic and therapeutic functions) [49–52]. Such efforts prompted the optimization of MSNs size, architecture and surface properties that include the application of stealth agents and/or targeting ligands to enhance MSNs biocompatibility, biodistribution and accumulation at the tumor site [53–55]. Furthermore, tracking agents such as quantum dots, iron oxide nanoparticles or fluorescent dyes have been also incorporated into MSNs to allow the monitoring of the nanoparticle fate in the human body. Simultaneously, MSNs can also be used to transport bioactive molecules and then deliver them to a specific target [56–58].

3.1. MSNs accumulation at the tumor tissue

The application of DDSs in cancer therapy can be impaired by a wide number of factors that modify the biodistribution and pharmacokinetic profile of the nanocarriers and subsequently limits their accumulation in tumor tissues. In fact, the nano-sized MSN-based systems can accumulate within tumor tissues through the EPR effect [59,60]. This effect is the result of the rapid tumor growth and simultaneous formation of new blood vessels. These newly formed blood vessels possess a leaky epithelium and a discontinuous microvasculature with fenestrations sizes of approximately 400 nm (this value can vary depending on the author) [61,62], therefore, nanoparticles with sizes inferior to these value are able to extravasate from the blood stream and accumulate in tumor tissue [63].

However, for a nanocarrier take advantage of the EPR effect, they must be able to avoid its rapid clearance and recognition by the reticuloendothelial system (RES) [64,65]. In the literature, it is described that nanocarriers with sizes inferior to 5 nm are rapidly cleared by renal filtration [66,67]. Moreover, those that have sizes lower than 50 nm will interact with the hepatocytes and become accumulated in the liver, whereas nanocarriers with sizes superior to 200 nm will be entrapped by the spleen and liver (please see Fig. 2) [66,67]. Accordingly, He et al. reported a gradual increase of MSNs accumulation in liver and spleen when the MSNs size increased from 80 to 360 nm [68]. To overcome such drawbacks,

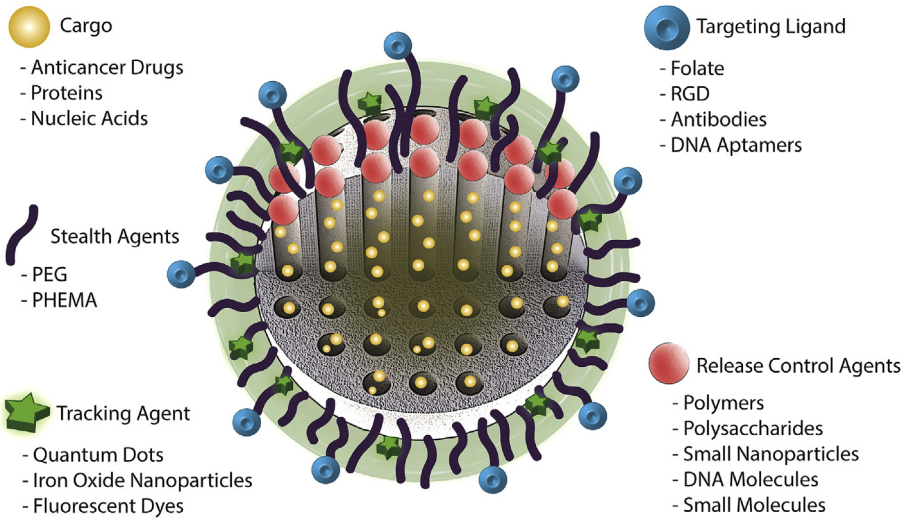

Fig. 1. Mesoporous silica nanoparticles multifunctionality and cargo loading possibilities. Different therapeutic biomolecules can be loaded into MSNs mesopores by adsorption from solution. Furthermore, different pore capping or blocking agents can be used to create stimuli responsive drug delivery MSNs based systems. Additionally, the MSNs surface can be modified with a polymer, such as PEG and PHEMA to imprint them stealth properties, avoiding its early elimination. The MSNs system can be further modified with targeting ligands (antibodies, small molecules, aptamers, etc.) to increase the particle specificity to the tumor tissue, and tracking agents (fluorescent dyes and contrast molecules) to allow the particle tracking and tumor imaging.

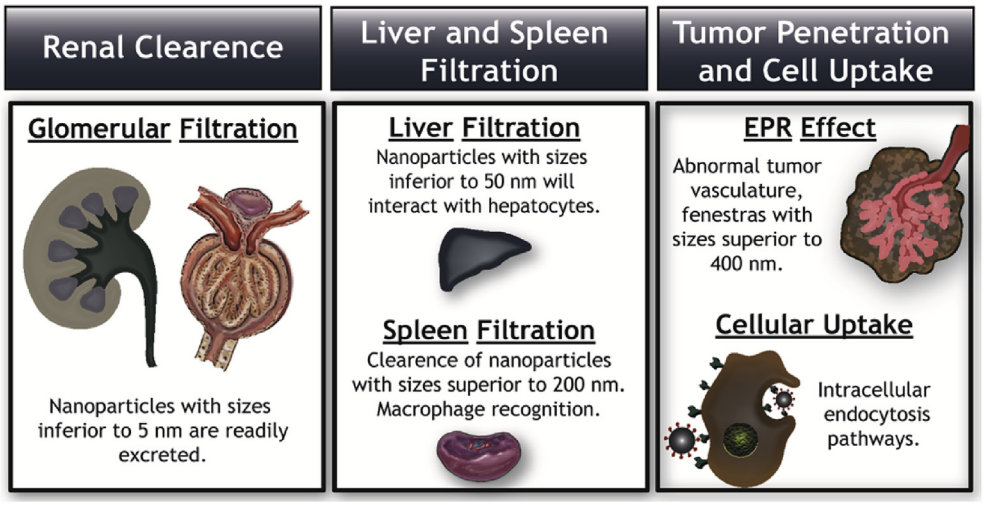

Fig. 2. Representation of the different barriers that the nanoparticles have to surpass during blood circulation. The nanoparticles must avoid renal, liver and spleen clearance to increase blood circulation times and the probability to accumulate in tumor tissue. Afterward, particles must be able to extravasate through the leaky tumor vasculature and ultimately interact with the target cells to exert its therapeutic effect.

MSNs functionalization with hydrophilic polymers (e.g., poly (ethylene glycol) (PEG) [69] and poly(2-hydroxyethyl methacrylate) (PHEMA) [70]) increase the nanocarrier blood circulation time, reduce the nanoparticle opsonization and avoid the formation of a protein corona on their surface, which is responsible for RES recognition and subsequent nanocarriers elimination [71]. In addition, He and coworkers also characterized the effect of MSNs PEGylation on the nonspecific protein binding, phagocytosis and hemolysis [72]. Their results revealed that the covalent grafting of PEG to MSNs surface avoids undesired interactions with biological components. They also disclosed that PEG, with a molecular weight of 10 000 Da and a density of 0.75%, is the best option to circumvent protein adsorption on MSNs surface, phagocytosis, and hemolysis when MSNs are used as DDSs. Moreover, the functionalization of MSNs with biologically active ligands such as antibodies (e.g., monoclonal antibody [73]), peptides (e.g., Arg-Gly-Asp (RGD) [74]), and small molecules (e.g., Folate [75]) can improve nanocarriers interaction with the target cells and augment their accumulation at the target site (see Fig. 1 for further details).

3.2. MSNs cellular uptake

One of the most important barriers that nanocarriers have to overcome to deliver drugs to target cells is the cell membrane. In mammalian cells, there are multiple pathways for DDSs be internalized by endocytosis, which can be further divided into two main categories, phagocytosis and pinocytosis [76]. Specialized cells (e.g. monocytes, macrophages and neutrophils) internalize large particles through phagocytosis, in a process that involves the engulfing of particles with sizes superior to 750 nm [77]. Alternatively, smaller particles, with sizes lower than 200–300 nm, are usually internalized through pinocytosis [76]. The pinocytosis can be further divided in clathrin-dependent, caveolin-dependent, receptor mediated, and clathrin- and caveolin-independent pathways (for a detailed review of the nanoparticles endocytosis process the readers are referred to [78]). The nanocarrier size, morphology and surface properties will impact on the internalization rate and the endocytic pathway used for MSNs transport into the cell cytoplasm. Zhu and coworkers evaluated the uptake pathways and entrance efficiency of MSNs produced with various sizes (55.6, 167.8 and 307.6 nm) [79]. Their results revealed that the endocytosis pathway and cellular uptake efficiency is size dependent, i.e. an increase in MSNs sizes lead to a decrease in their uptake efficiency. Furthermore, the size variation of MSNs also led to their cellular uptake through different endocytic pathways: clathrin-dependent via was used for larger MSNs; clathrin- and caveolin-dependent pathways were used for MSNs with 167.8 nm; while smaller particles used an energy independent pathway [79]. Slowing and colleagues described that the endocytosis mechanism used for MSNs internalization is also dependent on nanocarriers surface functionalization [80]. In their work, the MSNs were functionalized with fluorescein isothiocyanate (FITC-MSNs, zeta potential −34.73 mV), 3-aminopropyl (AP-MSNs, zeta potential −4.68 mV), guanidinopropyl (GP-MSNs, zeta potential −3.25 mV), 3-[N-(2-guanidinoethyl) guanidino]propyl (GEGP-MSNs, zeta potential +0.57 mV) and *N*-folate-3-aminopropyl (FAP-MSNs, zeta potential +12.81 mV) and then incubated with HeLa cells in the presence or absence of uptake pathways inhibitors. Their data revealed that the nanoparticles with most negative (FITC-MSNs) and the most positive (FAP-MSNs) zeta potential were the only ones to be internalized via clathrin-mediated mechanisms. Moreover, FAP-MSNs endocytosis was also mediated by folate receptors present at cells surface. The AP- and GP-MSNs uptake occurs through a caveolin-dependent mechanism, since the particles uptake was impaired by the caveolin inhibitors. Additionally, no mechanism of endocytosis was purposed for GEGP-MSNs since no change in their uptake was noticed when endocytic pathways inhibitors were used.

3.3. MSNs cytotoxic profile

A critical factor that affects nanocarrier application in biomedical applications is their biocompatibility. Despite the several studies performed so far for addressing MSNs biocompatibility, the mechanisms by which MSNs can lead, in certain cases, to cellular toxicity remain unclear [81–83]. The biocompatibility of these nanoparticles can be affected by several factors such as surface charge, particle size, morphology and porosity [84,85].

Nonetheless, the MSNs cytotoxicity has been associated to the presence of silanol groups (Si–OH) on their surface [83]. These groups can establish hydrogen bonds with the membrane components, or when they become dissociated ($Si–O^-$) interact with the

positively charged phospholipids [82,83]. Such interactions can cause cell lysis or at a phagosome level, induce the disruption of vesicle membrane and lead to the subsequent release of hydrolytic enzymes into the cytoplasm [82]. Further, the MSNs surface can induce the formation of reactive oxygen species (ROS), like the hydroxyl radical [86]. When they are present in low concentrations, the ROS can stimulate the production of inflammatory mediators that can promote mutagenesis and carcinogenesis [84,87]. However, at higher concentrations, these radical species have the capacity to disrupt cell membranes, damage the DNA molecules and promote cell apoptosis [88].

MSNs size can significantly impact their biocompatibility. However, contradictory information is found in literature, Slowing et al. reported that a decrease in MSNs size would lead to a reduced hemolysis of red blood cells (RBCs) [83], whereas Lin and Haynes reported a higher RBCs when the size of MSNs decrease from 260 to 25 nm [89]. Furthermore, the MSNs biocompatibility can also be dependent on the cell type. Yu and colleagues observed that RAW264.7 macrophage cells were more sensible to the MSNs exposition than A549 cancer cells, particularly for MSNs concentrations ranging from 250 to 500 μg/mL [82]. Notwithstanding, to date, various studies have shown that the MSNs are biocompatible with various types of mammalian cells, when concentrations lower than 200 μg/mL are used [82,90]. Moreover, it has been also reported that cell membrane integrity remains conserved after MSNs be uptaken and cells continue to display a normal morphology and mitochondrial activity [43,91,92].

The long-term biocompatibility, biodistribution, biodegradation and excretion of MSNs is not fully characterized. He and coworkers observed that mice injected with MSNs and PEGylated MSNs with different particle sizes (80, 120, 200 and 360 nm) survived for 1 month and no pathological abnormalities in the major organs were noticed [68]. Additionally, it was also reported that MSNs are excreted in urine and feces [55,93]. He and colleagues observed that 15–45% of the total injected amount of MSNs were excreted in urine, only 30 min post-injection [68]. However, a deeper characterization of MSNs biocompatibility is required, since modifications on MSNs particle geometry, porosity and surface features will affect the particles *in vivo* behavior.

4. Stimuli-responsive MSNs

The capacity to control the release profile and also to deliver a specific cargo to a target cell or tissue still remains one of the main challenges for the development of nano-sized carriers aimed for cancer therapy [94]. To accomplish such objectives, stimuli-responsive nanocarriers are currently being developed. Such systems allow a triggered release of a molecule in response to a local or external stimulus, such as pH, temperature, enzymatic, electromagnetic field, near infrared (NIR) radiation, redox potential, ultrasound and ATP (please see Fig. 3 for further details). This approach reduces drug interactions with healthy tissues during its circulation in the human body, thus contributing to the reduction of chemotherapy side effects. Therefore, a huge effort has been done for developing MSNs based systems capable of attaining a controlled and sustained delivery of bioactive molecules [95–97].

Taking into account that the drug reservoirs in MSNs are comprised by their tubular pores, the blocking of this structures with stimuli-responsive nanomaterials will prevent the drug premature release and subsequently, drug undesired interactions [98,99]. The controlled release of the cargo from MSNs-based systems can be achieved at three different levels (please see Fig. 4): i) coating particle surface [100], ii) pore sealing with molecular/particle gates [101], or iii) cargo coupling to the internal wall of the pore [102]. In turn, these three different approaches will rely on two types of response, the destruction or conformational change of the pore sealing agent or the use of labile/cleavable bonds that are broken upon stimulus exposition [43,103,104].

In the next topics, the approaches used to imprinting a stimuli responsiveness to the MSNs will be presented as well as the mechanisms of the drug release and its impact on the drugs release profile from these nanocarriers (a detailed list can be found in Table 1).

4.1. pH-responsive MSNs

The pH-responsive behavior is one of the most explored properties to design and produce nano-systems aimed for cancer therapy. The tumor microenvironment is characterized by pH values lower than the ones displayed by normal tissues. Such, can be attributed to the high cellular proliferative rate (e.g. increased acid lactic production), the increased efflux of intracellular protons (H^+) and low blood perfusion of tumor tissues [105,106]. Altogether, these factors lead to a decrease in oxygen content and a limited capacity to remove the acidic waste products resultant from metabolism [105]. Furthermore, at a subcellular level, in late endosomes and lysosomes, the nano-sized transporters can find even more acidic environments, with pH values ranging from 4.5 to 5.5 [107]. Therefore, this pH gradient has been explored for conferring specific drug release profiles to MSNs within tumor tissue.

Niedermayer and colleagues produced MSNs coated with poly(2-vinylpyridine) (PVP) and PEG and functionalized with acid folic to deliver doxorubicin (Dox) to T24 cancer cells [108]. Their results revealed that the incubation of PVP-coated MSNs at acidic pH values (pH 5.0) greatly promoted the cargo release, while at pH 7.4 only 4% of the cargo was released. This pH-dependent behavior of the particle is conferred by PVP protonation in contact with acidic environments, which will lead to the swelling of the polymeric matrix followed by cargo diffusion out of the pores. In a similar approach, Feng et al. developed a pH-responsive MSNs-based system by using an Alginate/Chitosan multilayer coating to perform drug delivery to HeLa cancer cells [109]. In their study, Dox was used as a model drug and the Alginate/Chitosan polyelectrolyte layers were assembled via electrostatic interaction in a process that involved their alternated deposition on MSNs surface. The *in vitro* assays revealed that an increased amount of drug was released, 7.5%–60.1%, when the pH was reduced from 7.4 to 4. Such result can be explained by the protonation of the chitosan NH_2 groups that leads to the swelling of the polymeric matrix and also to an increased electrostatic repulsion between the polymer and Dox molecules, thus promoting the drug diffusion through the polymeric coating to the external medium. Further, *in* vivo biodistribution assays performed in healthy rats demonstrated that the polyelectrolyte-coated MSNs limits Dox accumulation in major organs, which is fundamental to decrease the non-specific toxicity. Moreira et al. developed calcium carbonate coated MSNs for ibuprofen and Dox delivery to prostate cancer cells [43]. In their release experiments, the incubation of the coated MSNs at pH 7.4 showed a slow drug release, while at acidic pH a faster drug release was obtained. Such results can be explained by the rapid calcium carbonate dissociation into Ca^{2+} and CO_3^{2-}, when exposed to acidic media, whereas at physiological pH this material is relatively stable and present a much slower degradation rate. Moreover, when compared to the non-coated particles, the calcium carbonate coated MSNs favored the Dox accumulation in the cell nucleus and cytoplasm of prostate cancer cells, improving the drugs cytotoxic capacity.

One alternative to MSNs surface coating involves the utilization of pore capping agents that will confine the drugs into the interior

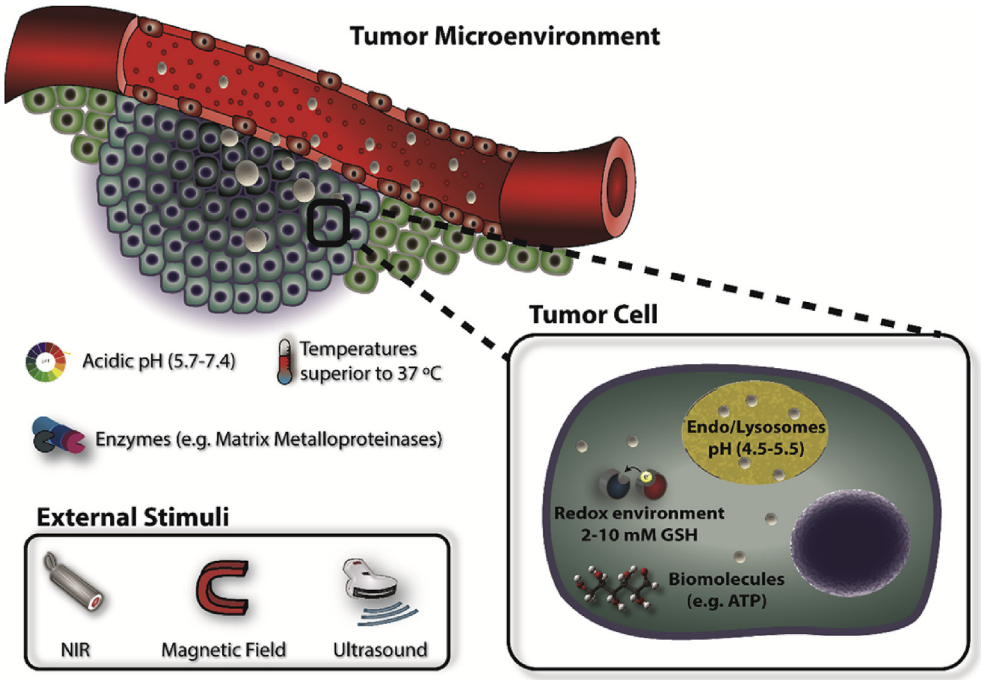

Fig. 3. Representation of the different stimuli that can be used to trigger the nanoparticle cargo release in the tumor tissue. The triggered release of the nanocarrier cargo in response to an environmental or external stimulus, present in the cancer tissue, will allow to avoid the host/drug interaction in healthy tissues and maximize the therapeutic effect.

of the pore. Yao and colleagues developed an acid sensitive capping agent based on PEGylated tetraphenylporphyrin zinc (Zn-Por-CA-PEG) and further modified the MSNs surface with histidine to deliver Dox to HeLa and MCF-7 cancer cells [110]. The pore capping agent was assembled by the formation of non-covalent bonds between the zinc on Zn-Por-CA-PEG molecules and the histidine grafted on MSNs surface. The release profile of these systems was characterized at pH values ranging from 5.3 to 7.4, revealing that as the pH decreases the amount of Dox released increase, reaching a maximum value of 80% at pH 5.3. This pH-dependent release profile results from the dissociation of the Zn-Por-CA-PEG/histidine complex at acidic pH values that promoted the pore uncapping and consequent Dox diffusion to the surrounding media. Consonantly, Chen and coworkers grafted ultra-small lanthanide doped nanoparticles with ultra-thin TaO_x layer (S-NPs) on the MSNs surface via acetals linkers to control the Dox delivery to HeLa cells (Fig. 5) [111]. In their approach, the acetal linker suffers hydrolysis at low pH values, allowing the removal of the S-NPs used to block the pore openings followed by drug release. Such behavior was confirmed through release experiments performed at different pH values. At pH 7.4 only 5% of the drug was released, while for pH 2.0 and 5.0 a pronounced Dox release was attained (about 90% and 60%, respectively). Moreover, in *in vivo* assays, the coated MSNs had a higher inhibitory effect on tumor growth and all the treated mice survived during the 30 days, which contrast with the 50% of mice survival rate obtained when free Dox was administered [111].

On the other hand, a controlled drug release from MSNs can also be achieved by promoting drug interactions with the pore wall. He and coworkers developed a pH-responsive MSNs based system to deliver Dox to MCF-7 cancer cells [112], where Dox was encapsulated in the interior of the CTAB micelles that acted as pore structuring agents during MSNs synthesis. The performed release experiments revealed that when MSNs were incubated at physiological pH Dox was scarcely released. In contrast, a completely different result was attained when MSNs were incubated in acidic media (pH 4 to 6.8), where a prompt release of Dox to the exterior medium was observed. The pH responsiveness presented by this system is originated by the electrostatic interactions that occur between the negatively charged silanol groups of MSNs and cationic quaternary ammonium cations available on CTAB micelles. When MSNs are in acidic environments they become less negative, leading to a reduction of the electrostatic interaction established between the MSNs and CTAB micelles and consequently a drug release to the exterior of the particle occurs. The *in vivo* application of Dox-loaded MSNs revealed that these nanoparticles besides being accumulated in tumor tissue, were also gathered by liver, spleen and lungs. Interestingly, the authors did not observe the Dox presence in the nucleus of normal cells, a fact attributed to the MSNs acidic dependent release behavior. A different approach was used by Lee and colleagues where Dox was linked to the internal pore surface of nanoparticles, previously modified with reactive hydrazone bonds [102]. For that purpose, the interior pore wall of MSNs was modified with aldehyde groups via triethoxysilylbutyraldehyde. Afterward, the aldehyde groups were reacted with hydrazide group from adipic acid dihydrazide to produce a reactive hydrazone bond. To immobilize Dox molecules inside the pores, the remaining hydrazide groups of adipic acid were reacted with the ketone group of Dox, originating an additional hydrazone bond. The utilization of this pH sensitive linker resulted in an unnoticeable Dox release at neutral pH, while MSNs incubation in acidic conditions (pH 1.0, 4.5 and 5.5) led to a pH-responsive Dox removal from the pore wall followed by its release to the surrounding medium. Further, cell studies performed in the presence or absence of bafilomycin A1 (BA) (a vacuolar type H^+-ATPase inhibitor that leads to an increased endosomal/lysosomal pH), revealed that the administration of Dox-loaded MSNs to HepG2 cells resulted in a cell viability of 30%, whereas when BA was present the cellular viability was near to 90%. Such results demonstrate the importance of the pH-responsive behavior of MSNs since the BA presence promoted

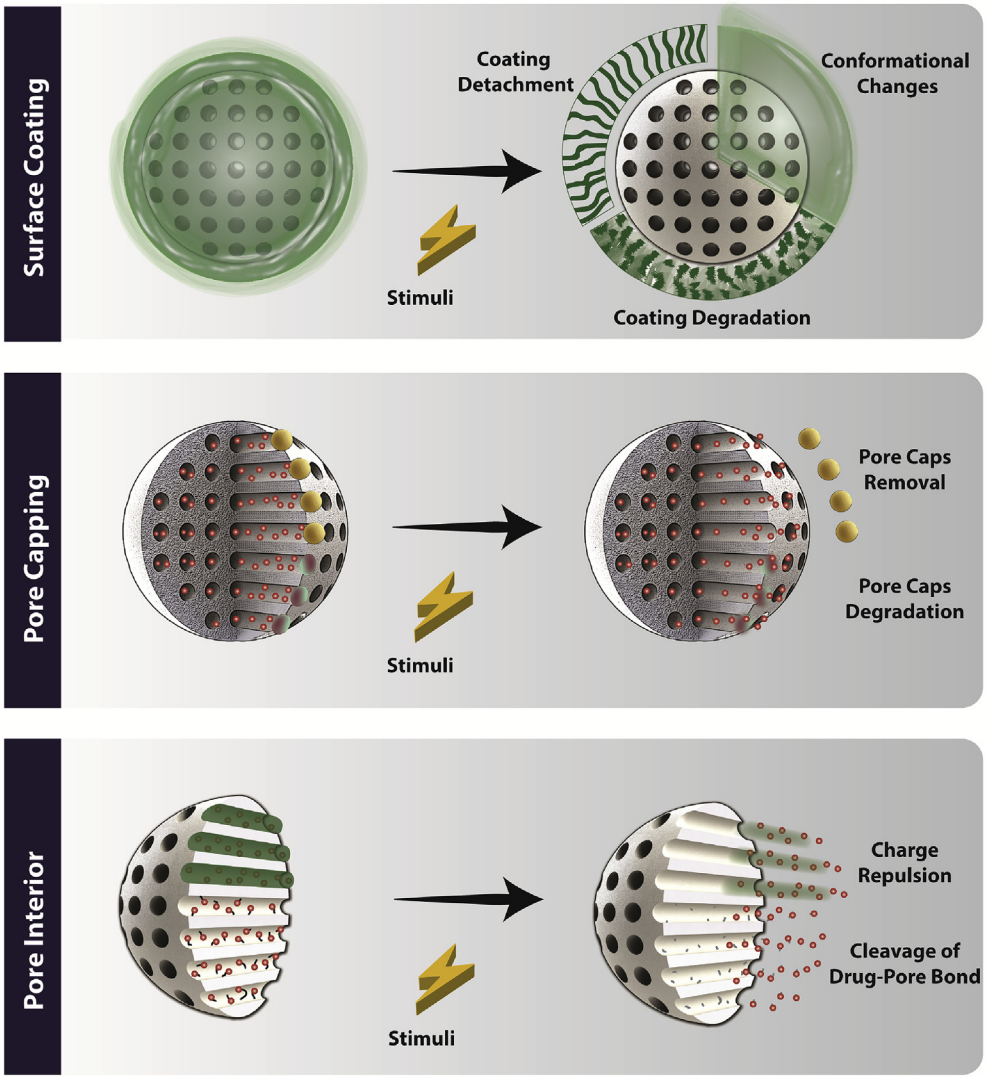

Fig. 4. Representation of the strategies utilized to create stimuli-responsive MSNs and the most common responses to the stimuli exposition. The stimuli responsiveness of MSNs can be achieved at three different levels, surface coating, pore capping or through drug interactions with internal pore wall. In turn, the changes that the stimuli exposition promote on MSNs will allow the drug diffusion to out of the pores.

the pH neutralization of endosomes/lysosomes and, consequently, the MSNs did not release the Dox inside cells.

4.2. Redox-triggered release

The redox responsive behavior of MSNs has also been studied for attaining a cargo controlled release. In the human body, the glutathione (GSH)/glutathione disulfide is one of the major redox couples that plays a relevant role in avoiding the damage caused by ROS species [113]. In fact, the GSH concentration in tumor cells is 100–1000 times superior to that found in the extracellular fluids [114,115]. Therefore, redox responsible nano-systems are aimed to disassemble and release their cargo in the cell cytoplasm, using as a trigger the redox potential [116]. Usually, redox responsive nano-systems incorporate a disulfide bond (general structure R–S–S–R) that is degraded in the presence of reducing agents, such as GSH [116,117].

One strategy employed for the production of redox responsive MSNs based systems is based on grafting polymers to the particle surface through disulfide bonds. Li and coworkers developed a redox-responsive MSN system by linking to the particle surface, through thiol bonds, a peptide containing an RGD sequence to deliver Dox to U87 MG cancer cells [74]. In their study, MSNs were initially incubated in a low reductive environment ([GSH] = 2 mM) and a Dox release of 33% was attained, while for a GSH concentration of 10 mM, a Dox release of 78% was determined. Such results suggest that the peptide incorporation on MSNs surface can block and control the drug release through a mechanism that involves thiol bonds degradation, in response to reductive environments. Consequently, peptide detachment from MSNs surface allows drug diffusion out of the pores. Moreover, cellular studies showed that the RGD functionalized MSNs had a higher cytotoxic effect on U87 MG cancer cells than the non-targeted counterparts. Furthermore, Sun and colleagues developed a Dox-loaded MSN-based system coated with oligo (ethylene glycol) acrylate crosslinked with *N, N′*-cystaminebismethacrylamide and then tested its application as DDS in African green monkey kidney cells transformed with a Simian Vacuolating Virus 40 (COS-7) cells [118]. The incubation of this system in a non-reductive environment promoted a drug release of 32%, whereas its incubation with 20 mM dithiothreitol

Table 1
Mesoporous silica nanoparticles (MSNs) stimuli responsive approaches: Therapeutic target, capping agent, MSNs physical properties before coating or capping and drug release mechanisms.

Stimuli	Approach	Therapeutic target	Type of test	Capping agent	MSNs physical parameters			Release mechanism	Ref.
					Size (nm)	Pore diameter (nm) and volume (cm^3/g)	Particle surface area (m^2/g)		
pH	Surface Coating	–	Proof of concept	Chitosan	110	Pore Diameter: 2.4 Pore Volume: 1.03	1020	Polymer conformational changes when exposed to acidic pH	[147]
		–	Proof of concept	Poly (4-vinyl pyridine)	n.d.	Pore Diameter: 2.5 Pore Volume: n.d.	640	Polymer conformational changes when exposed to acidic pH	[148]
		Cervical cancer	*In vitro* – HeLa cells	Coordination polymers of zinc and 1,4-bis (imidazol-1-ylmethyl) benzene (BIX)	100	Pore Diameter: 2.7 Pore Volume: 0.88	803	Coordination bonds between BIX and Zn are labile and dissociate at acidic pH	[149]
		Bladder cancer	*In vitro* – T24 cells	Poly (2-vinyl pyridine)	90	Pore Diameter: 3.78 Pore Volume: 0.79.	1097	Polymer conformational changes when exposed to acidic pH	[108]
		Cervical cancer	*In vitro* – HeLa cells *In vivo* – Sprague–Dawley rats (Biodistribution studies)	Alginate/chitosan polymer layers	110.2	Pore Diameter: 5.7 Pore Volume: n.d.	167.4	Polymer conformational changes when exposed to acidic pH	[109]
		Prostate cancer	*In vitro* – PC-3 cells	Calcium carbonate	156	Pore Diameter: 3.2 Pore Volume: 0.4	857	Calcium carbonate dissociation in acidic pH	[43]
	Pore Capping	–	Proof of concept	Fe_3O_4 nanoparticles	100	Pore Diameter: 3.6 Pore Volume: 1.15	1293	Acid-labile boronate ester linker	[150]
		Cervical and Breast cancer	*In vitro* – HeLa and MCF-7 cells	Zn-Por-CA-PEG/histidine complex	145	Pore Diameter: 2.32 Pore Volume: n.d.	1197	Dissociation of the Zn-Por-CA-PEG/histidine complex in acidic environments	[110]
		Liver cancer	*In vivo* – H22 tumor bearing Balb/c nude mice	Ultra-small lanthanide doped nanoparticles with ultra-thin TaOx layer (S-NPs)	n.d.	Pore Diameter: n.d. Pore Volume: n.d.	n.d.	S-NPs caps removal due to acetal linker hydrolysis in response to acidic environments	[111]
		Cervical cancer	*In vitro* – HeLa cells	ZnO quantum dots	100	Pore Diameter: 2.1 Pore Volume: n.d.	n.d.	Decomposition of ZnO quantum dots in acidic pH	[151]
		Cervical cancer	*In vitro* – HeLa cells	Gold nanoparticles	100	Pore Diameter: 3.9 Pore Volume: 1.75	1100	Electrostatic repulsion between Cysteine present in gold nanoparticles and NH^{3+} groups on MSNs surface	[34]
	Pore Interior	Breast cancer	*In vivo* – MCF-7 tumor bearing nude mice	CTAB micelles	112	Pore Diameter: n.d. Pore Volume: n.d.	n.d.	Electrostatic repulsion between CTAB micelles and MSNs pore wall at acidic pH	[112]
		Liver cancer	*In vitro* – HepG2 cells *In vivo* – Biodistribution studies on mice	Drug-MSNs pore wall grafting	100	Pore Diameter: 5.2 Pore Volume: 1.68	1265	Acid-labile hydrazone bond	[102]
Redox	Surface Coating	–	Proof of concept	PEG grafted via disulfide bonds	150	Pore Diameter: 2.9 Pore Volume: 0.9	1249	Redox sensible disulfide bond	[152]
		Brain cancer	*In vitro* – U87 MG cells	RGD sequence-containing peptide grafted via disulfide bonds	100	Pore Diameter: 2.64	1247	Redox sensible disulfide bond	[74]

Table 1 (*continued*)

Stimuli	Approach	Therapeutic target	Type of test	Capping agent	MSNs physical parameters			Release mechanism	Ref.
					Size (nm)	Pore diameter (nm) and volume (cm^3/g)	Particle surface area (m^2/g)		
						Pore Volume: n.d.			
		–	Proof of concept	oligo (ethylene glycol) acrylate crosslinked with N, N′-cystaminebismethacrylamide	n.d.	Pore Diameter: 3.5 Pore Volume: 0.58	667.9	Redox-sensitive disulfide polymer crosslinkers	[118]
	Pore Capping	Liver cancer	*In vivo* – HepG2 tumor bearing nude mice	Cytochrome C grafted to MSNs	160 –170	Pore Diameter: 3.29 Pore Volume: 0.63	768.89	Redox sensible disulfide bond	[120]
		Liver cancer	*In vitro* – HepG2 cells	MnO_2 nanostructures	120	Pore Diameter: 3.4 Pore Volume: 0.7	851.1	Redox responsive MnO_2 disassembly	[119]
		Cervical cancer	*In vitro* – HeLa cells	β-cyclodextrins grafted via disulfide bonds	100	Pore Diameter: 2.8 Pore Volume: n.d.	967	Redox sensible disulfide bond	[153]
ATP	Surface Coating	–	Proof of concept	ATP aptamer hybridized with ssDNA	80	Pore Diameter: 2.8 Pore Volume: 1	963.5	DNA coating dissociation via ATP-competitive binding	[122]
		Cervical cancer	*In vitro* – HeLa cells	Complexation between TDPA-Zn^{2+} and poly(Asp-Lys)-b-Asp	54.3	Pore Diameter: n.d. Pore Volume: n.d.	n.d.	Complex dissociation via ATP competitive binding to the TDPA-Zn^{2+}	[123]
Enzyme	Surface Coating	Breast cancer	*In vitro* – MDA-MB-231 cells	Poly (β-amino esters)	100	Pore Diameter: 2 Pore Volume: n.d.	1240	Esterase mediated coating degradation	[124]
		Liver cancer	*In vivo* – HepG2 tumor bearing nude mice	Serum albumin grafted via polypeptide linker	140	Pore Diameter: 3.61 Pore Volume: 0.80	888.55	Serum albumin detachment via linker recognition by MMP-2 enzyme	[125]
	Pore Capping	Cervical cancer	*In vitro* – HeLa cells	α-cyclodextrins grafted via azido-GFLGR7RGDS peptide	130	Pore Diameter: 3.86 Pore Volume: 1.10	1136.74	Capping removal via cathepsin B recognition and cleavage of the GFLG sequence	[126]
Temperature	Pore Capping	Breast cancer	*In vitro* – MDA-MB-231 cells	Zinc-doped iron oxide nanocrystal core and cucurbit[6]uril pore capping	255	Pore Diameter: n.d. Pore Volume: n.d.	n.d.	Capping removal when exposed to heat originated from magnetic field exposition	[136]
	Surface Coating	Cervical cancer	*In vitro* – HeLa cells	Poly(2-(dimethylamino) ethyl methacrylate)	100	Pore Diameter: 3.48 Pore Volume: 0.58	667.9	Polymer conformational changes in response to the temperature	[128]
		Breast cancer	*In vitro* – MCF-7 cells	DNA tagged copper sulfide nanospheres	58	Pore Diameter: n.d. Pore Volume: n.d.	n.d.	DNA melting when exposed to heat originated from NIR exposition	[132]
		Cervical cancer	*In vitro* – HeLa cells	DNA (hybridization of an oligonucleotide with an aptamer)	70 –120	Pore Diameter: n.d. Pore Volume: n.d.	n.d.	DNA melting when exposed to heat originated from NIR exposition	[131]
		Cervical and Breast cancer	*In vitro* – HeLa and MCF-7 cells	DNA (hybridization of an oligonucleotide with an aptamer)	58	Pore Diameter: n.d. Pore Volume: n.d.	n.d.	DNA melting when exposed to heat originated from NIR exposition	[134]
		–	Proof of concept	Maghemite nanocrystals and poly(ethyleneimine)-b-poly(N-	50 –100	Pore Diameter: 2.7	747		[135]

(*continued on next page*)

Table 1 (*continued*)

Stimuli	Approach	Therapeutic target	Type of test	Capping agent	MSNs physical parameters			Release mechanism	Ref.
					Size (nm)	Pore diameter (nm) and volume (cm^3/g)	Particle surface area (m^2/g)		
				isopropylacrylamide) copolymer coating		Pore Volume: n.d.		Polymer conformational changes when exposed to heat originated from magnetic field exposition	

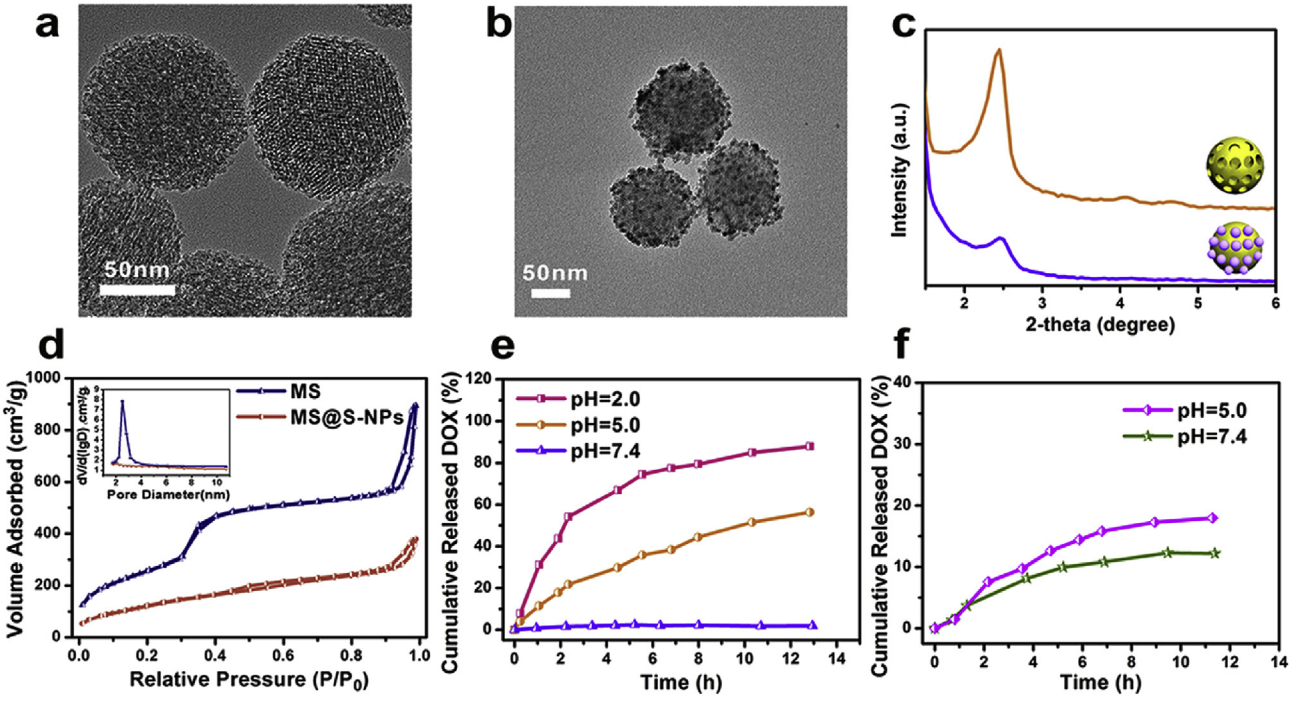

Fig. 5. TEM images of MSNs (a) and MSNs coated with S-NPs (b). Small angle powder X-ray diffraction of MSNs before (yellow) and after (purple) capping (c). Nitrogen adsorption-desorption isotherms and pore size distribution (inset) curves before and after capping (d). Cumulative release curves of Dox from MSNs coated with S-NPs (e) and MSNs (f) in buffer solutions at different pH. Reproduced from Ref. [111] with permission from Elsevier. (For interpretation of the references to colour in this figure legend, the reader is referred to the web version of this article.)

(DTT) prompted the release of 85% of Dox initially loaded. The incubation of MSNs with DTT promotes the rupture of the *N,N′*-cystaminebismethacrylamide disulfide bond (responsible for the polymers crosslinking and consequent pore blockage), that is fundamental for allowing the drug release from the nanoparticles. Further, the coating inclusion led to a reduction of protein adsorption on the surface of nanoparticles (23.4% and 3.4% of protein adsorption for bare MSNs and coated MSNs, respectively). Such is fundamental, since the opsonization of the nanoparticles is one of the main mechanisms used for nanocarriers clearance from the bloodstream. Additionally, cytotoxic assays revealed that the coated MSNs produced a cytotoxic effect similar to the free drug administration.

MSNs have been also functionalized with inorganic molecules. Yang and colleagues used manganese dioxide (MnO_2) nanostructures as capping agents for MSNs pore in order to confer them a redox-responsive behavior and also to allow a sustained Dox delivery to HepG2 cancer cells [119]. The exposition of this system to a reducing agent such as GSH leads to the reduction of MnO_2 to Mn^{2+}, which is responsible for triggering the coating disassembly followed by Dox release. The cellular studies revealed that MnO_2 coated MSNs have a higher cytotoxic effect to HepG2 cancer cells when compared to L02 cells. Such result is justified by the higher GSH content displayed by cancer cells, which promotes a faster Dox release leading to an increased cell death.

Another strategy used to control the drug release from MSNs involves the use of redox sensible pore caps that include small nanoparticles or molecular gatekeepers. Zhang and coworkers used cytochrome C molecules as pore-sealing agents in order to control Dox release (Fig. 6) [120]. The drug release assays were performed using fluorescein isothiocyanate as a model drug and they revealed that, in the presence of DTT, MSNs released 78.9% of the drug in only 3 h, while only 5.11% was attained in DTT absence. This difference can be explained by the disulfide bonds reduction and the cytochrome C caps removal that allow drug diffusion out of the pore, when MSNs are in contact with reductive environments. The *in vivo* experiments revealed that cytochrome C-capped MSNs loaded with Dox had the highest tumor inhibition (final tumor volume of 156 mm^3) among the test groups, free Dox (final tumor volume ~630 mm^3) and uncapped Dox-loaded MSNs (final tumor volume ~360 mm^3). Furthermore, along the time of the experiment no variations in nude mice body weight were observed for the cytochrome C-capped MSNs loaded with Dox, whereas the mice's treated with free Dox or uncapped Dox-loaded MSNs displayed an

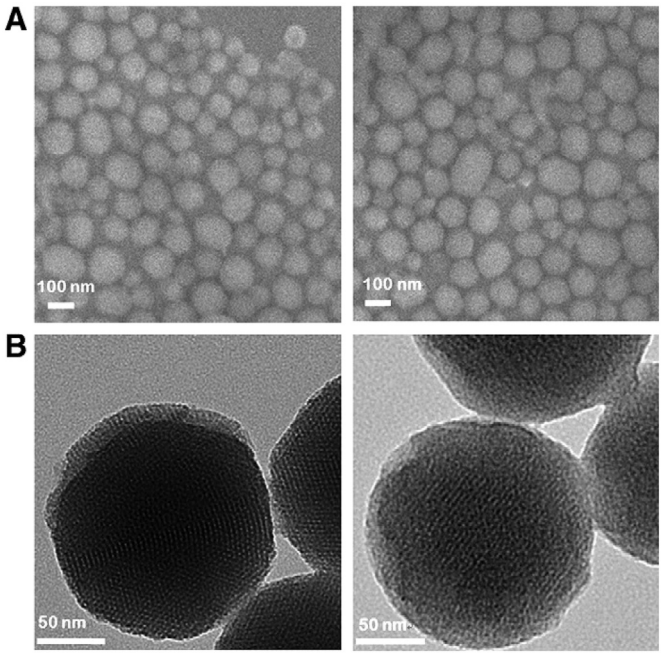

Fig. 6. Morphology characterization of MSNs: A) representative SEM images of MSNs–TPS (left) and MSNs–CytC–Apt (right); and B) representative TEM image of MSNs–TPS (left) and MSNs–CytC–Apt (right), respectively. Reproduced from Ref. [120] with permission from Elsevier.

obvious decrease in body weight. Such results show the importance of the gatekeeper for MSNs display an improved anti-tumoral capacity as well as to prevent unspecific body distribution and toxic side effects.

4.3. Adenosine triphosphate responsive approaches

MSNs responsive to ATP explore the gradient of ATP concentration that exists between the extracellular media and cell cytoplasm to trigger cargo release [121]. The ATP is one of the most important biomolecules in the cell and it is considered the universal currency used in intracellular energy transfer processes. ATP can be used as a trigger for cargo release since in the extracellular environment lower ATP concentrations (0.4 mM) are found in comparison to those available in the cytosol (1–10 mM) [121]. He and coworkers developed an ATP responsive MSNs formed through the hybridization of an ATP aptamer and two different single strands of DNA chains (ssDNA1 and ssDNA2) that were grafted to MSNs surface for drug delivery to Ramos cancer cells [122]. The release experiments performed in the absence of ATP showed a negligible cargo release, while the addition of ATP (20 mM) resulted in a release of 83.2% of the molecules loaded within MSNs. This behavior indicates that the DNA coating structure dissociates through a competitive binding between the ATP molecules and ATP aptamer that leads to the unblocking of the pores and allow the cargo diffusion. Moreover, the authors also verified that the amount of the cargo released was increased with the variation of ATP concentration until 5 mM, after this value, the release rate starts to stabilize and reaches its maximum when the ATP concentration attains 20 mM. In another work, Lai and coworkers developed a polypeptide-wrapped shell/core structured mesoporous silica/multicolor upconversion nanoparticles for Dox delivery to HeLa cancer cells [123]. The ATP responsiveness of their MSN based system was achieved by immobilizing a zinc-dipicolylamine analog (TDPA-Zn^{2+}) that interacts with the poly(Asp-Lys)-b-Asp peptidic coating. In their release experiments, it was verified that the presence of ATP promoted the fluorescein release. The produced nanoparticles were stable with a negligible (~4%) fluorescein release in the absence of ATP while the addition of increasing concentrations of ATP (1 mM, 5 mM, and 10 mM) greatly increased the amount of fluorescein released to ≈56%, ≈78% and ≈90, respectively. These results demonstrate that the ATP-competitive binding to the TDPA-Zn^{2+} complex promotes the polypeptide coating disassembly and cargo release.

4.4. Enzymatic dependent release

Another strategy used to achieve a site-specific drug release involves enzymes, which are available in the tumor tissue, for promoting the uncapping of MSNs and consequent cargo release. Therefore, these enzyme-responsive systems are designed to take advantage of the different intracellular and extracellular enzymes that are overexpressed or exhibit increased activity in tumor tissues. The utilization of enzymes as triggers to promote the drug release has been focused on the selection of MSNs surface coatings or pore capping/gatekeepers materials that can act as subtracts for enzymes. Fernando et al. grafted poly (β-amino esters) onto MSNs surface in order to obtain a controlled Dox release to MDA-MB-231 cancer cells, using an enzyme-mediated process [124]. The poly (β-amino ester) polymer was grafted through the establishment of a covalent bond between the polymer catechol groups and phenylboronic acid residues, previously introduced on MSNs surface. The incubation of this system with esterases resulted in a faster Dox release, reaching a maximum of 77%, which demonstrates that the ester groups were recognized by these enzymes and then hydrolyzed. Furthermore, the polymer coated MSNs displayed a similar cytotoxic effect to that of free Dox, which is explained by the high esterase concentrations present on cancer cells. In another study, Liu and coworkers used matrix metalloproteinase (MMP)-2 cleavable substrate polypeptide (PVGLIG) as a linker between MSNs and phenylboronic acid conjugated with human serum albumin coating [125]. Such procedure conferred to the carriers an enzymatic responsive character that allows them to perform the Dox delivery to HepG2 cancer cells. The release assays were performed using MMP-2 as the enzymatic trigger and the attained results revealed that after 24 h 73% of Dox was released from the nanoparticles, contrasting with the 17% of drug released when no enzyme was used. Such data shows that the MMP-2 enzyme can degrade the polypeptide (PVGLIG) linker, resulting in serum albumin coating removal and drug diffusion. Further, the *in vivo* application of these nanoparticles inhibited the hepatic tumor growth in mice and also displayed negligible toxic effects to normal organs. On the other side, the administration of free Dox or bare MSNs loaded with Dox displayed a smaller inhibitory effect on tumor growth and mice's weight decreased during the experiment time. Additionally, some degree of cardiotoxicity was observed for the test group treated with free Dox [125].

Cheng and colleagues used cyclodextrins as MSNs pore gatekeepers to control the Dox deliver to HeLa cancer cells [126]. To imprint the enzymatic responsive behavior to MSNs, the carriers were initially functionalized with γ-(2-aminoethyl)-aminopropyl trimethoxysilane for allowing a posterior modification with propargyl bromide originating MSNs-alkyne. Afterward, the enzyme sensitive pore gatekeepers, the azido-GFLGR_7RGDS peptide/α-cyclodextrins, were grafted by reacting them with the MSNs-alkyne. The incubation of this MSN system with cathepsin showed that 60% Dox was released in 24 h, whereas in cathepsin absence the release was only 10%. This result indicates that the cathepsin B recognize and cleaves the GFLG sequence present in the pore gatekeeper peptide causing its removal and consequent Dox

release. Moreover, in the cellular studies the pore capped MSNs presented a similar effect to free Dox administration (IC_{50} ~1.2 μg/mL and ~0.49 μg/mL, respectively). However, due to the RGD sequence present at MSNs surface in the pore gatekeeper, the MSNs possess some degree of selectivity to the $\alpha_v\beta_3$-integrins overexpressed by cancer cells.

4.5. Temperature responsive MSNs systems

The unique architecture of the tumor tissue originates an increment of the local temperature, giving the opportunity to explore the temperature difference between the tumor site and the surrounding healthy tissues to trigger a controlled release of the nanocarriers' cargo [98]. This temperature difference can result from the high cellular proliferation rate, abnormal vasculature and the presence of defective vascular nerve receptors found in the tumor tissues [127]. The abnormal tumor vasculature impairs the blood circulation through the tissue, which difficult the heat diffusion/removal from that area [19]. On the other side, the malfunctioning of the vascular nerve receptors hinders the effective temperature control by the nervous system. Therefore, to take advantage of this temperature increase it is desirable to design temperature-responsive drug carriers that only release drugs at temperatures above 37 °C, but confer drug protection while these systems are in blood circulation. Sun and colleagues developed poly(2-(dimethylamino) ethyl methacrylate)-coated MSNs for performing a temperature-dependent drug release to HeLa cancer cells [128]. The release experiments were performed using rhodamine B as a model drug and the obtained results revealed that the amount of drug released is proportional to the temperature increment. When incubated at 55 °C for 4 h about 80% of the encapsulated rhodamine was release. On the other side, when the MSNs were incubated at 45 and 30 °C the amount of rhodamine released decreased to 50 and 23%, respectively. This behavior is justified by the phase transition that the polymer shell suffers. When the temperature increases, the polymer chains shrink and rhodamine exits. Furthermore, the heating also accelerates rhodamine diffusion out of the pores by increasing its solubility.

Alternatively, the temperature differences between tumor and healthy tissues can be magnified by using external sources to create heat. Some materials based on carbon, copper, gold or others are capable of producing heat in response to specific wavelengths such as near infrared (NIR) radiation [129]. For biological applications, NIR is a very interesting alternative, since biological components such as proteins, melanin, hemoglobin, collagen and water present low or insignificant absorption of this radiation [130]. Furthermore, within the NIR region wavelength, three distinct regions have been identified as optimal (i.e. with wavelengths ranging from 700 to 950 nm, 1000–1350 nm and 1550–1870 nm), where each region presents an increased transparency against the biological components [131]. Zhang and coworkers developed MSNs coated with DNA tagged with copper sulfide nanospheres in order to develop a thermo-responsive Dox delivery system for HeLa and MCF-7 cancer cells [132]. For that purpose, the MSNs were functionalized with 3-aminopropyl triethoxysilane and then, an oligonucleotide was coupled to MSNs surface using succinimidyl 4-N-maleimidomethyl cyclohexane-1-carboxylate (SMCC) as crosslinker. The DNA-conjugated MSNs were mixed with the DNA tagged nanospheres to allow their hybridization, this DNA structure will block the pore openings and consequently entrap the Dox in the pore interior. The release assays revealed that the MSNs exposition to the NIR laser irradiation triggered the Dox release. Moreover, longer irradiation periods resulted in higher release rates. The release profile displayed by MSNs is justified by the generation of heat by the copper sulfide nanospheres when they are exposed to the NIR radiation, leading to the DNA melting and consequent Dox diffusion out of the pores. The cellular studies revealed that the administration of these nanocarriers, without being irradiated, to HeLa and MCF-7 cells did not have a pronounced cytotoxic effect (~70% of HeLa and ~95% of MCF-7 cells remained viable). However, upon laser irradiation for 30 s the HeLa and MCF-7 cell viabilities decreased to less than 10%, a result that can be explained by the faster Dox release and to the localized increase of temperature that can sensitize cancer cells to the Dox action as well as promote the inhibition of the cell DNA repair mechanisms, or even lead to cell necrosis when the temperature is superior to 45 °C [133].

Similarly, Zhang and colleagues developed a DNA-conjugated mesoporous silica coated with copper sulfide nanoparticles as a NIR-responsive delivery system of curcumin and Dox to MCF-7 and HeLa cancer cells [134]. To allow the DNA hybridization, the thiol modified oligonucleotide was grafted on amino-functionalized MSNs by using SMCC crosslinker. Afterward, the oligonucleotide-modified MSNs were incubated with a targeting AS1411 aptamer, allowing the AS1411 to hybridize with the oligonucleotide in order to a pore blocking structure be formed. The thermo-responsivity of this system was evaluated by performing assays with and without irradiation. The authors observed without NIR laser irradiation only 18% of Dox and 13% of curcumin were released. However, the irradiation of this system with NIR laser prompted the Dox and curcumin drug release (94 and 95%, respectively). These results indicate that the heat generated from the copper sulfide nucleus upon NIR laser irradiation leads to the denaturation of the DNA gatekeeper followed by drug diffusion from the MSNs. Further, in the cellular studies after NIR irradiation the MCF-7 and HeLa cells viability decreased to values lower than 20%, contrasting with the 60% cell viability observed for the cells exposed to the free drug administration.

On the other side, the use of external magnetic fields is an alternative approach capable of magnifying the local temperature in the tumor tissue. The use of magnetic fields as a trigger for a controlled release has an advantage over the use of NIR due to the better tissue penetration properties. Usually in this approaches, the MSNs have in its structure a magnetic responsive material (e.g. superparamagnetic iron oxide crystals) which produce heat when exposed to oscillating magnetic fields. Therefore, the resulting increase in the temperature is explored as the stimuli for the pore opening and allow the drug release. Baesa and coworkers developed a MSN-based drug delivery system with superparamagnetic maghemite nanocrystals entrapped within its structure and coated with poly(ethyleneimine)-b-poly(N-isopropylacrylamide) copolymer [135]. The release assays performed, using fluorescein as drug model, revealed that the exposition to an alternated magnetic field promotes the drug release reaching a final value of almost 50%, whereas in the absence of the magnetic field only a small leaching of the drug from MSNs was observed. Such behavior indicates that the local increase in temperature leads to a phase transition change on the polymeric coating, allowing the drug diffusion from the pores. Similarly, Thomas and colleagues developed a magnetic responsive MSN-based system comprised by a zinc-doped iron oxide nanocrystal core and a capping of cucurbit[6]uril to deliver Dox to MDA-MB-231 breast cancer cells [136]. The release assays revealed that the drug delivery occurs in response to magnetic field pulses. In fact, the authors observed that a single magnetic pulse was capable of promoting the release of 40% of the drug and when the particles were exposed to multiple pulses this value increased to about 95%. In contrast, only a negligible drug release occurs in the absence of a magnetic field. Such results indicate that the local internal heating promotes the removal of cucurbit[6]uril from the MSNs pore openings and allows the drug to diffuse out of the pores. Further, the cellular studies revealed that the combination of the

nanoparticle administration with the magnetic field exposition increased the cytotoxic capacity of the system, 35% of cell death, contrasting with the 5% observed in the absence of a magnetic field.

4.6. Multi-stimuli responsive MSNs

In addition to the abovementioned approaches, MSNs based systems can be engineered in order to be sensitive to more than one stimulus. These multi-stimuli responsive approaches combine the advantages of different single stimulus responsive strategies with the intent to enhance the spatial-temporal control of the cargo release. In fact, pH is one of the most exploited stimuli in multi-responsive MSNs and it has been used in combination with the enzymatic responsive mechanisms [137], temperature [138], glucose [139] or others. Chen and coworkers developed an MSNs-based delivery system capped with gold nanoparticles that were used to deliver Dox to HeLa cells. These nanocarriers were responsive to two different biological stimuli, pH and ATP [34]. Their results showed that the incubation of this gold capped MSNs in acidic pH's (4 and 4.5) prompted the cargo release, achieving a maximum of 90% at pH 4 and only 32% for pH 4.5. Moreover, the nanocarrier incubation at pH values superior to 5 resulted in an insignificant drug leakage. The pH responsivity of the gold capped MSNs is explained by the L-cysteine pH dependent charge. When the pH is higher than 5, L-cysteine is negatively charged and attracted to MSNs surface, leading to pore blockage. On the other hand, when the pH is inferior to 5, L-cysteine is protonated and a repulsion with the protonated MSNs surface occurs, that results in capping removal and subsequent drug release. Furthermore, upon addition of 10 mM ATP at pH 7, the MSNs cargo started to be released in a rapid way, in response to the gold nanoparticles capping removal through ATP chelation with Cu^{2+}. The *in vitro* assays revealed that the MSNs capped with gold nanoparticles displayed a similar cytotoxic effect to that of free drug (cell viability was ~50% after 24 h of drugs or MSNs administration).

In a different approach, Xiao and colleagues developed a pH and redox-responsive targeted MSNs nanocarrier for drug delivery to U87 cancer cells [140]. In their work, the MSNs were modified with (3-mercaptopropyl) trimethoxysilane and 2–2′-dithiodipyridine to produce MSN-S-S-Pyridine. Subsequently, RGDFFFFC peptide with an azide-terminal group was grafted onto the MSNs surface through the formation of a disulfide bond and the monomethoxy polyethylene glycol benzaldehyde polymer was linked to the peptide using click chemistry, to originate a stimulus responsive coating. In the release experiments, authors verified that an increase in DTT concentration leads to an increase in Dox release, reaching a maximum of 50% for 10 mM of DTT. Furthermore, the MSNs incubation at pH 5 in the absence of DTT resulted in a small release of Dox, while at pH 7.4 no distinguishable drug release was noticed. The nanocarrier redox responsive behavior (in the presence of DTT) is justified by the cleavage of the disulfide bonds that were formed between the peptide and MSNs surface, leading to a complete coating removal followed by Dox release from the carriers. When the particles are exposed to an acidic environment the benzoic-imine bond established between the peptide and PEG is hydrolyzed and, therefore, Dox leaks through the polymer/peptide coating. Furthermore, in *in vitro* assays, the coated MSNs displayed a pH dependent cytotoxicity, cell viability ranged from ~60% to ~25% at pH 7.4 and 5.0, respectively. Such result can be justified by the faster drug release when the pH and redox stimuli are present and the therapeutic effect is enhanced.

Other strategies can also be employed to create multi-responsive MSNs (Fig. 7) [141]. Jiao and colleagues developed MSNs that are responsive to redox environments and temperature, in order to control the Dox delivery to HeLa cancer cells [142]. The developed MSNs displayed a Dox release that was proportional to temperature, ranging from 10.6% at 37 °C, to 57.4% and 69.3% at 41 and 43 °C, respectively. Such results can be justified by the swollen state of the polymer shell, at low temperatures (≤37 °C), where the polymer is able to interact with drug and restrict their diffusion to the surrounding environment. In contrast, at higher temperatures the conformational changes that the polymer suffers decreases the polymer/drug interaction and also shortens the drug diffusion distance. Such allows a higher Dox release rate. Furthermore, the authors incubated the nanocarrier with 1 and 10 mM of GSH, at 37 °C, which resulted in a Dox release of 16.3% and 77.2%, respectively. The observed release profile indicates that the presence of a redox agent promotes the loosening or removal of polymer shell that results in drug diffusion from the MSNs. Additionally, the IC_{50} of coated MSNs loaded with Dox (640 ng/mL) is similar to that gathered with free Dox (578 ng/mL). Moreover, although not all the Dox-loaded on MSNs was released during the experiment, the particles presented a cytotoxic effect that is equivalent to that of free drug administration.

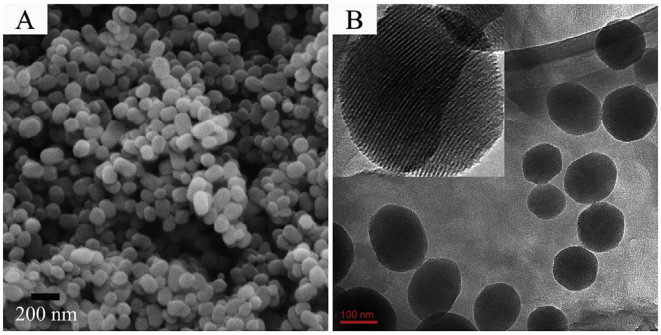

Fig. 7. SEM (A) and TEM (B) of MSN nanoparticles. Reproduced from Ref. [141] with permission from Elsevier.

4.7. Mathematical models used to simulate the drug release kinetics

The mathematical modeling allows the characterization of the drug release kinetics from the nanocarrier. Subsequently, the obtained *in silico* data can be used as a starting point to further optimize the developed MSN-based system. Usually, the drug release process can be divided into four main steps, the nanoparticles impregnation in the release medium, the drug dissolution, the drug diffusion through the particle matrix and the drug diffusion/convective transport in the release medium [143]. Despite the fact that in literature there are various mathematical models employed to analyze the release kinetics, the drug release profile for many DDSs can be modeled by applying the classic Fick's diffusion model or the Higuchi diffusion model [143,144]. Moreover, the majority of the MSNs drug delivery systems presents a release profile that follows the Higuchi diffusion model and can be divided into two main phases, an initial burst with a subsequent slow and controlled release [144]. Doadrio and colleagues reported that the erythromycin release profile from MSNs followed the Higuchi model when the release values were inferior to 50% [145]. Furthermore, Horcajada and coworkers observed that the ibuprofen release from the MSNs matrix had a linear relation with the one predicted by Higuchi model, with a regression factor (r value) superior to 0.99 [146]. Such behavior has been attributed to the physical and chemical entrapping of the drug within the MSNs pores. Further, the biomolecules diffusion to the outer medium occurs along time accordingly to the concentration gradient. Nevertheless, it is worth to notice that the modifications performed

on MSNs to imprint the stimuli-responsiveness can impact the release kinetics being important to evaluate and study each system individually.

5. Conclusion and future directions

In the present review, it was highlighted the MSNs potential to be used as stimuli-responsive anticancer DDSs. These systems can enhance drug solubility, avoid its premature degradation, sidestep drug interaction with healthy tissues, and ultimately, improve the drug bioavailability and therapeutic effectiveness. The strategies adopted by researchers to obtain a stimuli-sensitive drug release from MSNs include surface coating, pore capping, and pore interior functionalization. For that purpose, materials such as polymers, proteins, small molecules and inorganic components have been incorporated in MSNs to control the drug release. In turn, in response to stimuli present in the tumor the drug release from MSNs will occur due to the material degradation, conformational changes, detachment or charge repulsion. Moreover, the utilization of materials such gold and copper sulfide in these strategies also allows the combination of chemo- and thermo-therapies or even to perform real-time imaging (i.e. tumor visualization, particle tracking, etc.). Alternatively, the utilization of polymers (e.g. chitosan, PVP, PEG conjugates, etc.) or even protein-based approaches in addition to the stimuli responsiveness can enhance the biological performance of the MSNs by decreasing the protein adsorption, hemolysis, RES recognition, and their accumulation in healthy organs. Such can significantly impact on nanocarrier biocompatibility and therapeutic effectiveness.

In conclusion, nowadays, MSNs already have shown to be capable of keeping the drugs enclosed in its structure during blood circulation and, after reaching at the target site, release them in a highly controlled manner. Such controlled release can greatly reduce the undesirable side effects that currently limits the efficacy of antitumoral therapies. However, regardless of the advantageous versatility of these systems and the capacity to provide a very limited premature drug release, this DDSs often appear complicated and many still remain as proofs of concept. From this standpoint, it is still necessary to develop innovative methods for MSNs synthesis and functionalization that comply with the good manufacturing practice requirements in order to allow the technology transfer from lab to clinic. On the other side, as can be seen in Table 1, most of the MSNs-based systems in development are only evaluated using 2D cell cultures, which do not correlate with the real complexity of the tumors in the human body. Therefore, the MSNs real anti-tumoral capacity should be evaluated in more realistic *in vitro* models such as 3D cell cultures, which presents similar structure and cellular behavior to that observed on the real tissues. Further, the *in vivo* validation of MSNs-based systems is still required, mainly at the nanoparticles biodistribution, biodegradation, excretion and clearance level. In concordance to that the colloidal stability of MSNs in physiological media should also be studied in detail as well as the influence the administration route on the nanoparticle efficacy. The information that would be obtained from these extensive and comprehensive studies would allow the development of more well-designed MSNs-based approaches capable to reach the market, providing a novel generation of therapeutic agents more suitable for cancer application without the adverse side-effects.

Acknowledgments

This work is supported by FEDER funds through the POCI – COMPETE 2020 – Operational Programme Competitiveness and Internationalization in Axis I – Strengthening research, technological development and innovation (Project POCI-01-0145-FEDER-007491) and National Funds by FCT – Foundation for Science and Technology (Project UID/Multi /00709/2013). André F. Moreira acknowledges individual Ph.D. fellowship from FCT (SFRH/BD/109482/2015).

References

[1] V.M. Gaspar, A.F. Moreira, E.C. Costa, J.A. Queiroz, F. Sousa, C. Pichon, I.J. Correia, Gas-generating TPGS-PLGA microspheres loaded with nanoparticles (NIMPS) for co-delivery of minicircle DNA and anti-tumoral drugs, Colloids Surf. B 134 (2015) 287–294.
[2] T. Wang, H. Zhu, J. Zhuo, Z. Zhu, P. Papakonstantinou, G. Lubarsky, J. Lin, M. Li, Biosensor based on ultrasmall MoS2 nanoparticles for electrochemical detection of H_2O_2 released by cells at the nanomolar level, Anal. Chem. 85 (2013) 10289–10295.
[3] S. Santra, P. Zhang, K. Wang, R. Tapec, W. Tan, Conjugation of biomolecules with luminophore-doped silica nanoparticles for photostable biomarkers, Anal. Chem. 73 (2001) 4988–4993.
[4] G. Tian, X. Zheng, X. Zhang, W. Yin, J. Yu, D. Wang, Z. Zhang, X. Yang, Z. Gu, Y. Zhao, TPGS-stabilized $NaYbF_4$:Er upconversion nanoparticles for dual-modal fluorescent/CT imaging and anticancer drug delivery to overcome multi-drug resistance, Biomaterials 40 (2015) 107–116.
[5] J.G. Marques, V.M. Gaspar, E. Costa, C.M. Paquete, I.J. Correia, Synthesis and characterization of micelles as carriers of non-steroidal anti-inflammatory drugs (NSAID) for application in breast cancer therapy, Colloids Surf. B 113 (2014) 375–383.
[6] Y. Liu, S. An, J. Li, Y. Kuang, X. He, Y. Guo, H. Ma, Y. Zhang, B. Ji, C. Jiang, Brain-targeted co-delivery of therapeutic gene and peptide by multifunctional nanoparticles in Alzheimer's disease mice, Biomaterials 80 (2016) 33–45.
[7] R. Huang, H. Ma, Y. Guo, S. Liu, Y. Kuang, K. Shao, J. Li, Y. Liu, L. Han, S. Huang, S. An, L. Ye, J. Lou, C. Jiang, Angiopep-conjugated nanoparticles for targeted long-term gene therapy of Parkinson's disease, Pharm. Res. 30 (2013) 2549–2559.
[8] G. Kibria, H. Hatakeyama, H. Harashima, Cancer multidrug resistance: mechanisms involved and strategies for circumvention using a drug delivery system, Arch. Pharm. Res. 37 (2014) 4–15.
[9] A. Albanese, P.S. Tang, W.C. Chan, The effect of nanoparticle size, shape, and surface chemistry on biological systems, Annu. Rev. Biomed. Eng. 14 (2012) 1–16.
[10] J. Lu, Z. Li, J.I. Zink, F. Tamanoi, In vivo tumor suppression efficacy of mesoporous silica nanoparticles-based drug-delivery system: enhanced efficacy by folate modification, Nanomed. (N. Y., N. Y. U. S.) 8 (2012) 212–220.
[11] Y. Sun, W. Zou, S. Bian, Y. Huang, Y. Tan, J. Liang, Y. Fan, X. Zhang, Bioreducible PAA-g-PEG graft micelles with high doxorubicin loading for targeted antitumor effect against mouse breast carcinoma, Biomaterials 34 (2013) 6818–6828.
[12] M.J. Ernsting, M. Murakami, A. Roy, S.D. Li, Factors controlling the pharmacokinetics, biodistribution and intratumoral penetration of nanoparticles, J. Control. Release 172 (2013) 782–794.
[13] R. Lehner, X. Wang, M. Wolf, P. Hunziker, Designing switchable nanosystems for medical application, J. Control. Release 161 (2012) 307–316.
[14] A. Wicki, D. Witzigmann, V. Balasubramanian, J. Huwyler, Nanomedicine in cancer therapy: challenges, opportunities, and clinical applications, J. Control. Release 200 (2015) 138–157.
[15] E. Phillips, O. Penate-Medina, P.B. Zanzonico, R.D. Carvajal, P. Mohan, Y.P. Ye, J. Humm, M. Gonen, H. Kalaigian, H. Schoder, H.W. Strauss, S.M. Larson, U. Wiesner, M.S. Bradbury, Clinical translation of an ultrasmall inorganic optical-PET imaging nanoparticle probe, Sci. Transl. Med. 6 (2014).
[16] I. Slowing, J.L. Vivero-Escoto, C.W. Wu, V.S. Lin, Mesoporous silica nanoparticles as controlled release drug delivery and gene transfection carriers, Adv. Drug Deliv. Rev. 60 (2008) 1278–1288.
[17] J.L. Vivero-Escoto, I. Slowing, B.G. Trewyn, V.S. Lin, Mesoporous silica nanoparticles for intracellular controlled drug delivery, Small 6 (2010) 1952–1967.
[18] J.M. Rosenholm, C. Sahlgren, M. Linden, Towards multifunctional, targeted drug delivery systems using mesoporous silica nanoparticles–opportunities & challenges, Nanoscale 2 (2010) 1870–1883.
[19] S. Baek, R.K. Singh, D. Khanal, K.D. Patel, E.J. Lee, K.W. Leong, W. Chrzanowski, H.W. Kim, Smart multifunctional drug delivery towards anticancer therapy harmonized in mesoporous nanoparticles, Nanoscale 7 (2015) 14191–14216.
[20] H. Mekaru, J. Lu, F. Tamanoi, Development of mesoporous silica-based nanoparticles with controlled release capability for cancer therapy, Adv. Drug Deliv. Rev. 95 (2015) 40–49.
[21] Y. Tian, A. Glogowska, W. Zhong, T. Klonisch, M. Xing, Polymeric mesoporous silica nanoparticles as a pH-responsive switch to control doxorubicin intracellular delivery, J. Mater. Chem. B 1 (2013) 5264–5272.
[22] L. Xiong, X. Du, B.Y. Shi, J.X. Bi, F. Kleitz, S.Z. Qiao, Tunable stellate mesoporous silica nanoparticles for intracellular drug delivery, J. Mater. Chem. B 3 (2015) 1712–1721.

[23] L. Xiong, X. Du, F. Kleitz, S.Z. Qiao, Cancer-cell-specific nuclear-targeted drug delivery by dual-ligand-modified mesoporous silica nanoparticles, Small 11 (2015) 5919–5926.
[24] L. Li, T. Liu, C. Fu, L. Tan, X. Meng, H. Liu, Biodistribution, excretion, and toxicity of mesoporous silica nanoparticles after oral administration depend on their shape, Nanomed. (N. Y., N. Y. U. S.) 11 (2015) 1915–1924.
[25] T. Liu, L. Li, X. Teng, X. Huang, H. Liu, D. Chen, J. Ren, J. He, F. Tang, Single and repeated dose toxicity of mesoporous hollow silica nanoparticles in intravenously exposed mice, Biomaterials 32 (2011) 1657–1668.
[26] W. Stöber, A. Fink, E. Bohn, Controlled growth of monodisperse silica spheres in the micron size range, J. Colloid Interface Sci. 26 (1968) 62–69.
[27] M. Grun, I. Lauer, K.K. Unger, The synthesis of micrometer- and submicrometer-size spheres of ordered mesoporous oxide MCM-41, Adv. Mater. 9 (1997) 254.
[28] M.T. Harris, R.R. Brunson, C.H. Byers, The base-catalyzed-hydrolysis and condensation-reactions of dilute and concentrated teos solutions, J. Non Cryst. Solids 121 (1990) 397–403.
[29] S.H. Wu, C.Y. Mou, H.P. Lin, Synthesis of mesoporous silica nanoparticles, Chem. Soc. Rev. 42 (2013) 3862–3875.
[30] D. Douroumis, I. Onyesom, M. Maniruzzaman, J. Mitchell, Mesoporous silica nanoparticles in nanotechnology, Crit. Rev. Biotechnol. 33 (2013) 229–245.
[31] Z. Li, J.C. Barnes, A. Bosoy, J.F. Stoddart, J.I. Zink, Mesoporous silica nanoparticles in biomedical applications, Chem. Soc. Rev. 41 (2012) 2590–2605.
[32] F. Tang, L. Li, D. Chen, Mesoporous silica nanoparticles: synthesis, biocompatibility and drug delivery, Adv. Mater. 24 (2012) 1504–1534.
[33] Y. Wang, Q.F. Zhao, N. Han, L. Bai, J. Li, J. Liu, E.X. Che, L. Hu, Q. Zhang, T.Y. Jiang, S.L. Wang, Mesoporous silica nanoparticles in drug delivery and biomedical applications, Nanomed. (N. Y., N. Y. U. S.) 11 (2015) 313–327.
[34] X. Chen, X.Y. Cheng, A.H. Soeriyadi, S.M. Sagnella, X. Lu, J.A. Scott, S.B. Lowe, M. Kavallaris, J.J. Gooding, Stimuli-responsive functionalized mesoporous silica nanoparticles for drug release in response to various biological stimuli, Biomater. Sci. 2 (2014) 121–130.
[35] C. Charnay, S. Begu, C. Tourne-Peteilh, L. Nicole, D.A. Lerner, J.M. Devoisselle, Inclusion of ibuprofen in mesoporous templated silica: drug loading and release property, Eur. J. Pharm. Biopharm. 57 (2004) 533–540.
[36] F. Gao, P. Botella, A. Corma, J. Blesa, L. Dong, Monodispersed mesoporous silica nanoparticles with very large pores for enhanced adsorption and release of DNA, J. Phys. Chem. B 113 (2009) 1796–1804.
[37] S.B. Hartono, W.Y. Gu, F. Kleitz, J. Liu, L.Z. He, A.P.J. Middelberg, C.Z. Yu, G.Q. Lu, S.Z. Qiao, Poly-L-lysine functionalized large pore cubic mesostructured silica nanoparticles as biocompatible carriers for gene delivery, Acs Nano 6 (2012) 2104–2117.
[38] M.H. Kim, H.K. Na, Y.K. Kim, S.R. Ryoo, H.S. Cho, K.E. Lee, H. Jeon, R. Ryoo, D.H. Min, Facile synthesis of monodispersed mesoporous silica nanoparticles with ultralarge pores and their application in gene delivery, Acs Nano 5 (2011) 3568–3576.
[39] I.I. Slowing, B.G. Trewyn, V.S.Y. Lin, Mesoporous silica nanoparticles for intracellular delivery of membrane-impermeable proteins, J. Am. Chem. Soc. 129 (2007) 8845–8849.
[40] J. Moraes, K. Ohno, T. Maschmeyer, S. Perrier, Synthesis of silica-polymer core-shell nanoparticles by reversible addition-fragmentation chain transfer polymerization, Chem. Commun. 49 (2013) 9077–9088.
[41] J.W. Park, Y.J. Park, C.H. Jun, Post-grafting of silica surfaces with pre-functionalized organosilanes: new synthetic equivalents of conventional trialkoxysilanes, Chem. Commun. 47 (2011) 4860–4871.
[42] J.L. Townson, Y.S. Lin, J.O. Agola, E.C. Carnes, H.S. Leong, J.D. Lewis, C.L. Haynes, C.J. Brinker, Re-examining the size/charge paradigm: differing in vivo characteristics of size- and charge-matched mesoporous silica nanoparticles, J. Am. Chem. Soc. 135 (2013) 16030–16033.
[43] A.F. Moreira, V.M. Gaspar, E.C. Costa, D. de Melo-Diogo, P. Machado, C.M. Paquete, I.J. Correia, Preparation of end-capped pH-sensitive mesoporous silica nanocarriers for on-demand drug delivery, Eur. J. Pharm. Biopharm. 88 (2014) 1012–1025.
[44] W. Ngamcherdtrakul, J. Morry, S. Gu, D.J. Castro, S.M. Goodyear, T. Sangvanich, M.M. Reda, R. Lee, S.A. Mihelic, B.L. Beckman, Z. Hu, J.W. Gray, W. Yantasee, Cationic polymer modified mesoporous silica nanoparticles for targeted SiRNA delivery to HER2+ breast cancer, Adv. Funct. Mater. 25 (2015) 2646–2659.
[45] L. Mu, S.S. Feng, A novel controlled release formulation for the anticancer drug paclitaxel (Taxol): PLGA nanoparticles containing vitamin E TPGS, J. Control. Release 86 (2003) 33–48.
[46] A.J. Primeau, A. Rendon, D. Hedley, L. Lilge, I.F. Tannock, The distribution of the anticancer drug Doxorubicin in relation to blood vessels in solid tumors, Clin. Cancer Res. 11 (2005) 8782–8788.
[47] M.A. Izquierdo, R.H. Shoemaker, M.J. Flens, G.L. Scheffer, L. Wu, T.R. Prather, R.J. Scheper, Overlapping phenotypes of multidrug resistance among panels of human cancer-cell lines, Int. J. Cancer 65 (1996) 230–237.
[48] S. Kunjachan, B. Rychlik, G. Storm, F. Kiessling, T. Lammers, Multidrug resistance: physiological principles and nanomedical solutions, Adv. Drug Deliv. Rev. 65 (2013) 1852–1865.
[49] M. Yu, S. Jambhrunkar, P. Thorn, J. Chen, W. Gu, C. Yu, Hyaluronic acid modified mesoporous silica nanoparticles for targeted drug delivery to CD44-overexpressing cancer cells, Nanoscale 5 (2013) 178–183.
[50] F. Chen, H. Hong, S. Goel, S.A. Graves, H. Orbay, E.B. Ehlerding, S. Shi, C.P. Theuer, R.J. Nickles, W. Cai, In vivo tumor vasculature targeting of CuS@MSN based theranostic nanomedicine, Acs Nano 9 (2015) 3926–3934.
[51] F. Chen, T. Nayak, H. Hong, S. Graves, R. Nickles, W.B. Cai, In vivo tumor targeting with dual-labeled mesoporous silica nanoparticles, J. Nucl. Med. 55 (2014).
[52] M.Y. Wu, Q.S. Meng, Y. Chen, P.F. Xu, S.J. Zhang, Y.P. Li, L.X. Zhang, M. Wang, H.L. Yao, J.L. Shi, Ultrasmall confined iron oxide nanoparticle MSNs as a pH-responsive theranostic platform, Adv. Funct. Mater. 24 (2014) 4273–4283.
[53] X.L. Huang, L.L. Li, T.L. Liu, N.J. Hao, H.Y. Liu, D. Chen, F.Q. Tang, The shape effect of mesoporous silica nanoparticles on biodistribution, clearance, and biocompatibility in vivo, Acs Nano 5 (2011) 5390–5399.
[54] H. Meng, M. Xue, T. Xia, Z. Ji, D.Y. Tarn, J.I. Zink, A.E. Nel, Use of size and a copolymer design feature to improve the biodistribution and the enhanced permeability and retention effect of doxorubicin-loaded mesoporous silica nanoparticles in a murine xenograft tumor model, Acs Nano 5 (2011) 4131–4144.
[55] J. Lu, M. Liong, Z. Li, J.I. Zink, F. Tamanoi, Biocompatibility, biodistribution, and drug-delivery efficiency of mesoporous silica nanoparticles for cancer therapy in animals, Small 6 (2010) 1794–1805.
[56] F.F. Zheng, P.H. Zhang, Y. Xi, J.J. Chen, L.L. Li, J.J. Zhu, Aptamer/graphene quantum dots nanocomposite capped fluorescent mesoporous silica nanoparticles for intracellular drug delivery and real-time monitoring of drug release, Anal. Chem. 87 (2015) 11739–11745.
[57] S. Zhou, D.Q. Huo, C.J. Hou, M. Yang, H.B. Fa, C. Xia, M. Chen, Mesoporous silica-coated quantum dots functionalized with folic acid for lung cancer cell imaging, Anal. Methods 7 (2015) 9649–9654.
[58] X. Huang, F. Zhang, S. Lee, M. Swierczewska, D.O. Kiesewetter, L. Lang, G. Zhang, L. Zhu, H. Gao, H.S. Choi, G. Niu, X. Chen, Long-term multimodal imaging of tumor draining sentinel lymph nodes using mesoporous silica-based nanoprobes, Biomaterials 33 (2012) 4370–4378.
[59] J. Fang, H. Nakamura, H. Maeda, The EPR effect: unique features of tumor blood vessels for drug delivery, factors involved, and limitations and augmentation of the effect, Adv. Drug Deliv. Rev. 63 (2011) 136–151.
[60] L. Tang, N.P. Gabrielson, F.M. Uckun, T.M. Fan, J. Cheng, Size-dependent tumor penetration and in vivo efficacy of monodisperse drug-silica nanoconjugates, Mol. Pharm. 10 (2013) 883–892.
[61] F. Danhier, O. Feron, V. Preat, To exploit the tumor microenvironment: passive and active tumor targeting of nanocarriers for anti-cancer drug delivery, J. Control. Release 148 (2010) 135–146.
[62] F. Alexis, E. Pridgen, L.K. Molnar, O.C. Farokhzad, Factors affecting the clearance and biodistribution of polymeric nanoparticles, Mol. Pharm. 5 (2008) 505–515.
[63] J.D. Byrne, T. Betancourt, L. Brannon-Peppas, Active targeting schemes for nanoparticle systems in cancer therapeutics, Adv. Drug Deliv. Rev. 60 (2008) 1615–1626.
[64] V. Torchilin, Tumor delivery of macromolecular drugs based on the EPR effect, Adv. Drug Deliv. Rev. 63 (2011) 131–135.
[65] U. Prabhakar, H. Maeda, R.K. Jain, E.M. Sevick-Muraca, W. Zamboni, O.C. Farokhzad, S.T. Barry, A. Gabizon, P. Grodzinski, D.C. Blakey, Challenges and key considerations of the enhanced permeability and retention effect for nanomedicine drug delivery in oncology, Cancer Res. 73 (2013) 2412–2417.
[66] B. Wang, X. He, Z. Zhang, Y. Zhao, W. Feng, Metabolism of nanomaterials in vivo: blood circulation and organ clearance, Acc. Chem. Res. 46 (2013) 761–769.
[67] R.K. Jain, T. Stylianopoulos, Delivering nanomedicine to solid tumors, Nat. Rev. Clin. Oncol. 7 (2010) 653–664.
[68] Q. He, Z. Zhang, F. Gao, Y. Li, J. Shi, In vivo biodistribution and urinary excretion of mesoporous silica nanoparticles: effects of particle size and PEGylation, Small 7 (2011) 271–280.
[69] H. Meng, W.X. Mai, H. Zhang, M. Xue, T. Xia, S. Lin, X. Wang, Y. Zhao, Z. Ji, J.I. Zink, A.E. Nel, Codelivery of an optimal drug/siRNA combination using mesoporous silica nanoparticles to overcome drug resistance in breast cancer in vitro and in vivo, Acs Nano 7 (2013) 994–1005.
[70] Y. Zhu, H.S. Sundaram, S. Liu, L. Zhang, X. Xu, Q. Yu, J. Xu, S. Jiang, A robust graft-to strategy to form multifunctional and stealth zwitterionic polymer-coated mesoporous silica nanoparticles, Biomacromolecules 15 (2014) 1845–1851.
[71] Q. Dai, C. Walkey, W.C. Chan, Polyethylene glycol backfilling mitigates the negative impact of the protein corona on nanoparticle cell targeting, Angew. Chem. 53 (2014) 5093–5096.
[72] Q. He, J. Zhang, J. Shi, Z. Zhu, L. Zhang, W. Bu, L. Guo, Y. Chen, The effect of PEGylation of mesoporous silica nanoparticles on nonspecific binding of serum proteins and cellular responses, Biomaterials 31 (2010) 1085–1092.
[73] F. Chen, H. Hong, Y. Zhang, H.F. Valdovinos, S. Shi, G.S. Kwon, C.P. Theuer, T.E. Barnhart, W. Cai, In vivo tumor targeting and image-guided drug delivery with antibody-conjugated, radiolabeled mesoporous silica nanoparticles, Acs Nano 7 (2013) 9027–9039.
[74] Z.-Y. Li, J.-J. Hu, Q. Xu, S. Chen, H.-Z. Jia, Y.-X. Sun, R.-X. Zhuo, X.-Z. Zhang, A redox-responsive drug delivery system based on RGD containing peptide-capped mesoporous silica nanoparticles, J. Mater. Chem. B 3 (2015) 39–44.
[75] F. Porta, G.E. Lamers, J. Morrhayim, A. Chatzopoulou, M. Schaaf, H. den Dulk, C. Backendorf, J.I. Zink, A. Kros, Folic acid-modified mesoporous silica nanoparticles for cellular and nuclear targeted drug delivery, Adv. Healthc. Mater. 2 (2013) 281–286.

[76] S. Mayor, R.E. Pagano, Pathways of clathrin-independent endocytosis, Nat. Rev. Mol. Cell Biol. 8 (2007) 603–612.
[77] H. Ishimoto, K. Yanagihara, N. Araki, H. Mukae, N. Sakamoto, K. Izumikawa, M. Seki, Y. Miyazaki, Y. Hirakata, Y. Mizuta, K. Yasuda, S. Kohno, Single-cell observation of phagocytosis by human blood dendritic cells, Jpn. J. Infect. Dis. 61 (2008) 294–297.
[78] T.G. Iversen, T. Skotland, K. Sandvig, Endocytosis and intracellular transport of nanoparticles: present knowledge and need for future studies, Nano Today 6 (2011) 176–185.
[79] J. Zhu, L. Liao, L. Zhu, P. Zhang, K. Guo, J. Kong, C. Ji, B. Liu, Size-dependent cellular uptake efficiency, mechanism, and cytotoxicity of silica nanoparticles toward HeLa cells, Talanta 107 (2013) 408–415.
[80] I. Slowing, B.G. Trewyn, V.S. Lin, Effect of surface functionalization of MCM-41-type mesoporous silica nanoparticles on the endocytosis by human cancer cells, J. Am. Chem. Soc. 128 (2006) 14792–14793.
[81] X. Huang, L. Li, T. Liu, N. Hao, H. Liu, D. Chen, F. Tang, The shape effect of mesoporous silica nanoparticles on biodistribution, clearance, and biocompatibility in vivo, Acs Nano 5 (2011) 5390–5399.
[82] T. Yu, A. Malugin, H. Ghandehari, Impact of silica nanoparticle design on cellular toxicity and hemolytic activity, Acs Nano 5 (2011) 5717–5728.
[83] I. Slowing, C.W. Wu, J.L. Vivero-Escoto, V.S. Lin, Mesoporous silica nanoparticles for reducing hemolytic activity towards mammalian red blood cells, Small 5 (2009) 57–62.
[84] T. Asefa, Z. Tao, Biocompatibility of mesoporous silica nanoparticles, Chem. Res. Toxicol. 25 (2012) 2265–2284.
[85] D. Tarn, C.E. Ashley, M. Xue, E.C. Carnes, J.I. Zink, C.J. Brinker, Mesoporous silica nanoparticle nanocarriers: biofunctionality and biocompatibility, Acc. Chem. Res. 46 (2013) 792–801.
[86] M.A.A. Schoonen, C.A. Cohn, E. Roemer, R. Laffers, S.R. Simon, T. O'Riordan, Mineral-induced formation of reactive oxygen species, Rev. Mineral. Geochem. 64 (2006) 179–221.
[87] S.I. Grivennikov, F.R. Greten, M. Karin, Immunity, inflammation, and cancer, Cell 140 (2010) 883–899.
[88] R.K. Kankala, Y. Kuthati, C.L. Liu, C.Y. Mou, C.H. Lee, Killing cancer cells by delivering a nanoreactor for inhibition of catalase and catalytically enhancing intracellular levels of ROS, RSC Adv. 5 (2015) 86072–86081.
[89] Y.S. Lin, C.L. Haynes, Impacts of mesoporous silica nanoparticle size, pore ordering, and pore integrity on hemolytic activity, J. Am. Chem. Soc. 132 (2010) 4834–4842.
[90] S.P. Hudson, R.F. Padera, R. Langer, D.S. Kohane, The biocompatibility of mesoporous silicates, Biomaterials 29 (2008) 4045–4055.
[91] T.H. Chung, S.H. Wu, M. Yao, C.W. Lu, Y.S. Lin, Y. Hung, C.Y. Mou, Y.C. Chen, D.M. Huang, The effect of surface charge on the uptake and biological function of mesoporous silica nanoparticles in 3T3-L1 cells and human mesenchymal stem cells, Biomaterials 28 (2007) 2959–2966.
[92] S. Lee, H.S. Yun, S.H. Kim, The comparative effects of mesoporous silica nanoparticles and colloidal silica on inflammation and apoptosis, Biomaterials 32 (2011) 9434–9443.
[93] J.S. Souris, C.H. Lee, S.H. Cheng, C.T. Chen, C.S. Yang, J.A. Ho, C.Y. Mou, L.W. Lo, Surface charge-mediated rapid hepatobiliary excretion of mesoporous silica nanoparticles, Biomaterials 31 (2010) 5564–5574.
[94] P. Couvreur, Nanoparticles in drug delivery: past, present and future, Adv. Drug Deliv. Rev. 65 (2013) 21–23.
[95] Z. Li, D.L. Clemens, B.Y. Lee, B.J. Dillon, M.A. Horwitz, J.I. Zink, Mesoporous silica nanoparticles with pH-sensitive nanovalves for delivery of moxifloxacin provide improved treatment of lethal pneumonic tularemia, Acs Nano 9 (2015) 10778–10789.
[96] J.L. Paris, M.V. Cabanas, M. Manzano, M. Vallet-Regi, Polymer-grafted mesoporous silica nanoparticles as ultrasound-responsive drug carriers, Acs Nano 9 (2015) 11023–11033.
[97] L. Palanikumar, E.S. Choi, J.Y. Cheon, S.H. Joo, J.H. Ryu, Noncovalent polymer-gatekeeper in mesoporous silica nanoparticles as a targeted drug delivery platform, Adv. Funct. Mater. 25 (2015) 957–965.
[98] M. Colilla, B. Gonzalez, M. Vallet-Regi, Mesoporous silica nanoparticles for the design of smart delivery nanodevices, Biomater. Sci. 1 (2013) 114–134.
[99] Y. Sun, H. Sai, K.A. Spoth, K.W. Tan, U. Werner-Zwanziger, J. Zwanziger, S.M. Gruner, L.F. Kourkoutis, U. Wiesner, Stimuli-responsive shapeshifting mesoporous silica nanoparticles, Nano Lett. 16 (2016) 651–655.
[100] Y. Zhang, C.Y. Ang, M. Li, S.Y. Tan, Q. Qu, Z. Luo, Y. Zhao, Polymer-coated hollow mesoporous silica nanoparticles for triple-responsive drug delivery, Acs Appl. Mater. Interfaces 7 (2015) 18179–18187.
[101] N. Song, Y.W. Yang, Molecular and supramolecular switches on mesoporous silica nanoparticles, Chem. Soc. Rev. 44 (2015) 3474–3504.
[102] C.H. Lee, S.H. Cheng, I.P. Huang, J.S. Souris, C.S. Yang, C.Y. Mou, L.W. Lo, Intracellular pH-responsive mesoporous silica nanoparticles for the controlled release of anticancer chemotherapeutics, Angew. Chem. 49 (2010) 8214–8219.
[103] Y. Zhao, J.L. Vivero-Escoto, Slowing II, B.G. Trewyn, V.S. Lin, Capped mesoporous silica nanoparticles as stimuli-responsive controlled release systems for intracellular drug/gene delivery, Expert Opin. Drug Deliv. 7 (2010) 1013–1029.
[104] H. Peng, R. Dong, S. Wang, Z. Zhang, M. Luo, C. Bai, Q. Zhao, J. Li, L. Chen, H. Xiong, A pH-responsive nano-carrier with mesoporous silica nanoparticles cores and poly(acrylic acid) shell-layers: fabrication, characterization and properties for controlled release of salidroside, Int. J. Pharm. 446 (2013) 153–159.
[105] E.S. Lee, Z. Gao, Y.H. Bae, Recent progress in tumor pH targeting nanotechnology, J. Control. Release 132 (2008) 164–170.
[106] D. Hanahan, R.A. Weinberg, Hallmarks of cancer: the next generation, Cell 144 (2011) 646–674.
[107] L.E. Gerweck, K. Seetharaman, Cellular pH gradient in tumor versus normal tissue: potential exploitation for the treatment of cancer, Cancer Res. 56 (1996) 1194–1198.
[108] S. Niedermayer, V. Weiss, A. Herrmann, A. Schmidt, S. Datz, K. Muller, E. Wagner, T. Bein, C. Brauchle, Multifunctional polymer-capped mesoporous silica nanoparticles for pH-responsive targeted drug delivery, Nanoscale 7 (2015) 7953–7964.
[109] W. Feng, W. Nie, C. He, X. Zhou, L. Chen, K. Qiu, W. Wang, Z. Yin, Effect of pH-responsive alginate/chitosan multilayers coating on delivery efficiency, cellular uptake and biodistribution of mesoporous silica nanoparticles based nanocarriers, Acs Appl. Mater. Interfaces 6 (2014) 8447–8460.
[110] X.M. Yao, X.F. Chen, C.L. He, L. Chen, X.S. Chen, Dual pH-responsive mesoporous silica nanoparticles for efficient combination of chemotherapy and photodynamic therapy, J. Mater. Chem. B 3 (2015) 4707–4714.
[111] Y. Chen, K. Ai, J. Liu, G. Sun, Q. Yin, L. Lu, Multifunctional envelope-type mesoporous silica nanoparticles for pH-responsive drug delivery and magnetic resonance imaging, Biomaterials 60 (2015) 111–120.
[112] Q. He, Y. Gao, L. Zhang, Z. Zhang, F. Gao, X. Ji, Y. Li, J. Shi, A pH-responsive mesoporous silica nanoparticles-based multi-drug delivery system for overcoming multi-drug resistance, Biomaterials 32 (2011) 7711–7720.
[113] J.M. Estrela, A. Ortega, E. Obrador, Glutathione in cancer biology and therapy, Crit. Rev. Clin. Lab. Sci. 43 (2006) 143–181.
[114] R. Cheng, F. Feng, F. Meng, C. Deng, J. Feijen, Z. Zhong, Glutathione-responsive nano-vehicles as a promising platform for targeted intracellular drug and gene delivery, J. Control. Release 152 (2011) 2–12.
[115] F.Q. Schafer, G.R. Buettner, Redox environment of the cell as viewed through the redox state of the glutathione disulfide/glutathione couple, Free Radicals Biol. Med. 30 (2001) 1191–1212.
[116] S. Ganta, H. Devalapally, A. Shahiwala, M. Amiji, A review of stimuli-responsive nanocarriers for drug and gene delivery, J. Control. Release 126 (2008) 187–204.
[117] M. Huo, J. Yuan, L. Tao, Y. Wei, Redox-responsive polymers for drug delivery: from molecular design to applications, Polym. Chem. 5 (2014) 1519–1528.
[118] J.T. Sun, J.G. Piao, L.H. Wang, M. Javed, C.Y. Hong, C.Y. Pan, One-pot synthesis of redox-responsive polymers-coated mesoporous silica nanoparticles and their controlled drug release, Macromol. Rapid Commun. 34 (2013) 1387–1394.
[119] X. Yang, D.G. He, X.X. He, K.M. Wang, Z. Zou, X.C. Li, H. Shi, J.R. Luo, X.X. Yang, Glutathione-mediated degradation of surface-capped MnO_2 for drug release from mesoporous silica nanoparticles to cancer cells, Part. Part. Syst. Charact. 32 (2015) 205–212.
[120] B. Zhang, Z. Luo, J. Liu, X. Ding, J. Li, K. Cai, Cytochrome c end-capped mesoporous silica nanoparticles as redox-responsive drug delivery vehicles for liver tumor-targeted triplex therapy in vitro and in vivo, J. Control. Release 192 (2014) 192–201.
[121] R. Mo, T. Jiang, R. DiSanto, W. Tai, Z. Gu, ATP-triggered anticancer drug delivery, Nat. Commun. 5 (2014) 3364.
[122] X. He, Y. Zhao, D. He, K. Wang, F. Xu, J. Tang, ATP-responsive controlled release system using aptamer-functionalized mesoporous silica nanoparticles, Langmuir 28 (2012) 12909–12915.
[123] J. Lai, B.P. Shah, Y. Zhang, L. Yang, K.B. Lee, Real-time monitoring of ATP-responsive drug release using mesoporous-silica-coated multicolor upconversion nanoparticles, Acs Nano 9 (2015) 5234–5245.
[124] I.R. Fernando, D.P. Ferris, M. Frasconi, D. Malin, E. Strekalova, M.D. Yilmaz, M.W. Ambrogio, M.M. Algaradah, M.P. Hong, X. Chen, M.S. Nassar, Y.Y. Botros, V.L. Cryns, J.F. Stoddart, Esterase- and pH-responsive poly(beta-amino ester)-capped mesoporous silica nanoparticles for drug delivery, Nanoscale 7 (2015) 7178–7183.
[125] J. Liu, B. Zhang, Z. Luo, X. Ding, J. Li, L. Dai, J. Zhou, X. Zhao, J. Ye, K. Cai, Enzyme responsive mesoporous silica nanoparticles for targeted tumor therapy in vitro and in vivo, Nanoscale 7 (2015) 3614–3626.
[126] Y.J. Cheng, G.F. Luo, J.Y. Zhu, X.D. Xu, X. Zeng, D.B. Cheng, Y.M. Li, Y. Wu, X.Z. Zhang, R.X. Zhuo, F. He, Enzyme-induced and tumor-targeted drug delivery system based on multifunctional mesoporous silica nanoparticles, Acs Appl. Mater. Interfaces 7 (2015) 9078–9087.
[127] G. Lorusso, C. Ruegg, The tumor microenvironment and its contribution to tumor evolution toward metastasis, Histochem. Cell Biol. 130 (2008) 1091–1103.
[128] J.T. Sun, Z.Q. Yu, C.Y. Hong, C.Y. Pan, Biocompatible zwitterionic sulfobetaine copolymer-coated mesoporous silica nanoparticles for temperature-responsive drug release, Macromol. Rapid Commun. 33 (2012) 811–818.
[129] H.J. Cho, M. Chung, M.S. Shim, Engineered photo-responsive materials for near-infrared-triggered drug delivery, J. Ind. Eng. Chem. 31 (2015) 15–25.
[130] J. Eichler, J. Knof, H. Lenz, Measurements on the depth of penetration of light (0.35–1.0 microgram) in tissue, Radiat. Environ. Biophys. 14 (1977) 239–242.
[131] E. Hemmer, A. Benayas, F. Légaré, F. Vetrone, Exploiting the biological windows: current perspectives on fluorescent bioprobes emitting above 1000 nm, Nanoscale Horiz. 1 (2016) 168–184.

[132] L. Zhang, Y. Li, Z. Jin, J.C. Yu, K.M. Chan, An NIR-triggered and thermally responsive drug delivery platform through DNA/copper sulfide gates, Nanoscale 7 (2015) 12614–12624.
[133] D. Jaque, L. Martinez Maestro, B. del Rosal, P. Haro-Gonzalez, A. Benayas, J.L. Plaza, E. Martin Rodriguez, J. Garcia Sole, Nanoparticles for photothermal therapies, Nanoscale 6 (2014) 9494–9530.
[134] Y. Zhang, Z. Hou, Y. Ge, K. Deng, B. Liu, X. Li, Q. Li, Z. Cheng, P. Ma, C. Li, J. Lin, DNA-hybrid-gated photothermal mesoporous silica nanoparticles for NIR-responsive and aptamer-targeted drug delivery, Acs Appl. Mater. Interfaces 7 (2015) 20696–20706.
[135] A. Baeza, E. Guisasola, E. Ruiz-Hernandez, M. Vallet-Regi, Magnetically triggered multidrug release by hybrid mesoporous silica nanoparticles, Chem. Mater 24 (2012) 517–524.
[136] C.R. Thomas, D.P. Ferris, J.H. Lee, E. Choi, M.H. Cho, E.S. Kim, J.F. Stoddart, J.S. Shin, J. Cheon, J.I. Zink, Noninvasive remote-controlled release of drug molecules in vitro using magnetic actuation of mechanized nanoparticles, J. Am. Chem. Soc. 132 (2010) 10623–10625.
[137] A. Hakeem, R. Duan, F. Zahid, C. Dong, B. Wang, F. Hong, X. Ou, Y. Jia, X. Lou, F. Xia, Dual stimuli-responsive nano-vehicles for controlled drug delivery: mesoporous silica nanoparticles end-capped with natural chitosan, Chem. Commun. 50 (2014) 13268–13271.
[138] X. Wu, Z. Wang, D. Zhu, S. Zong, L. Yang, Y. Zhong, Y. Cui, pH and thermo dual-stimuli-responsive drug carrier based on mesoporous silica nanoparticles encapsulated in a copolymer-lipid bilayer, Acs Appl. Mater. Interfaces 5 (2013) 10895–10903.
[139] M.D. Yilmaz, M. Xue, M.W. Ambrogio, O. Buyukcakir, Y. Wu, M. Frasconi, X. Chen, M.S. Nassar, J.F. Stoddart, J.I. Zink, Sugar and pH dual-responsive mesoporous silica nanocontainers based on competitive binding mechanisms, Nanoscale 7 (2015) 1067–1072.
[140] D. Xiao, H.Z. Jia, J. Zhang, C.W. Liu, R.X. Zhuo, X.Z. Zhang, A dual-responsive mesoporous silica nanoparticle for tumor-triggered targeting drug delivery, Small 10 (2014) 591–598.
[141] Q. Zhao, J. Liu, W. Zhu, C. Sun, D. Di, Y. Zhang, P. Wang, Z. Wang, S. Wang, Dual-stimuli responsive hyaluronic acid-conjugated mesoporous silica for targeted delivery to CD44-overexpressing cancer cells, Acta Biomater. 23 (2015) 147–156.
[142] Y. Jiao, Y. Sun, B. Chang, D. Lu, W. Yang, Redox- and temperature-controlled drug release from hollow mesoporous silica nanoparticles, Chemistry 19 (2013) 15410–15420.
[143] J. Siepmann, F. Siepmann, Mathematical modeling of drug delivery, Int. J. Pharm. 364 (2008) 328–343.
[144] S.B. Wang, Ordered mesoporous materials for drug delivery, Micropor. Mesopor. Mat. 117 (2009) 1–9.
[145] J.C. Doadrio, E.M.B. Sousa, I. Izquierdo-Barba, A.L. Doadrio, J. Perez-Pariente, M. Vallet-Regi, Functionalization of mesoporous materials with long alkyl chains as a strategy for controlling drug delivery pattern, J. Mater. Chem. 16 (2006) 462–466.
[146] P. Horcajada, A. Ramila, J. Perez-Pariente, M. Vallet-Regi, Influence of pore size of MCM-41 matrices on drug delivery rate, Micropor. Mesopor. Mat. 68 (2004) 105–109.
[147] A. Popat, J. Liu, G.Q. Lu, S.Z. Qiao, A pH-responsive drug delivery system based on chitosan coated mesoporous silica nanoparticles, J. Mater. Chem. 22 (2012) 11173–11178.
[148] R. Liu, P. Liao, J. Liu, P. Feng, Responsive polymer-coated mesoporous silica as a pH-sensitive nanocarrier for controlled release, Langmuir 27 (2011) 3095–3099.
[149] L. Xing, H. Zheng, Y. Cao, S. Che, Coordination polymer coated mesoporous silica nanoparticles for pH-responsive drug release, Adv. Mater. 24 (2012) 6433–6437.
[150] Q. Gan, X. Lu, Y. Yuan, J. Qian, H. Zhou, X. Lu, J. Shi, C. Liu, A magnetic, reversible pH-responsive nanogated ensemble based on Fe_3O_4 nanoparticles-capped mesoporous silica, Biomaterials 32 (2011) 1932–1942.
[151] F. Muhammad, M. Guo, W. Qi, F. Sun, A. Wang, Y. Guo, G. Zhu, pH-Triggered controlled drug release from mesoporous silica nanoparticles via intracelluar dissolution of ZnO nanolids, J. Am. Chem. Soc. 133 (2011) 8778–8781.
[152] Z. Xie, H. Gong, M. Liu, H. Zhu, H. Sun, The properties of mesoporous silica nanoparticles functionalized with different PEG-chain length via the disulfide bond linker and drug release in glutathione medium, J. Biomater. Sci. Polym. Ed. 27 (2016) 55–68.
[153] Q. Zhang, F. Liu, K.T. Nguyen, X. Ma, X.J. Wang, B.G. Xing, Y.L. Zhao, Multifunctional mesoporous silica nanoparticles for cancer-targeted and controlled drug delivery, Adv. Funct. Mater. 22 (2012) 5144–5156.